

3. MIDDLE EOCENE TO MIOCENE CALCAREOUS NANNOFOSSILS OF LEG 125 FROM THE WESTERN PACIFIC OCEAN¹

Yulin Xu^{2,3} and Sherwood W. Wise, Jr.²

ABSTRACT

During Ocean Drilling Program Leg 125, a thick sequence of middle Eocene to Pleistocene pelagic sediments, volcanogenic sediments, and predominantly extrusive volcanic rocks was recovered. Calcareous nannofossils were examined from 15 holes at nine sites, but Eocene to Miocene calcareous nannofossils were found only from Holes 782A, 784A, 786A, and 786B. In portions of Holes 786A and 786B, datable nannofossil oozes were found intercalated among volcanic flows. The nannofossil biostratigraphy of these holes indicates the presence of three well-defined hiatuses: within the lower Oligocene, between the upper Oligocene and middle Miocene, and between the middle and upper Miocene.

An attempt was made to correlate the magnetostratigraphical data with the first or last occurrences of the following species: *Sphenolithus distentus*, *Reticulofenestra bisecta*, *Reticulofenestra reticulata*, and *Cyclicargolithus floridanus abisectus* n. comb. The results indicate that the FO of *Sphenolithus distentus* can extend down to Zone CP16 (34.7 Ma), the LO of *Reticulofenestra bisecta* best defines the boundary between CP19a and CP19b (23.5 Ma), and the LO of *Cyclicargolithus f. abisectus* n. comb. can extend up to Subzone CN5a (12.5 Ma). No latest Oligocene *Cyclicargolithus f. abisectus* n. comb. acme was observed. *Cyclicargolithus abisectus* is considered a subspecies or variant of *Cyclicargolithus floridanus* because their LOs coincide. As a consequence of these observations, we have modified the definitions of Bukry's Subzones CP14a, CP14b, and CN1a.

Analyses of sediment-accumulation rates indicate that the rates increased gradually from the Eocene to Miocene. This is especially evident since the late Miocene in Hole 782A. In different parts of the Izu-Bonin forearc basin, however, the rate is not everywhere the same and appears to vary according to the import of volcanogenic materials.

INTRODUCTION

The Bonin-Mariana region is made up of a complex series of arcs and basins formed since the start of westward subduction of Pacific lithosphere in the Eocene. The evolution of these arc and basin systems is thought to have begun in the early-middle Eocene, and development of the system continued through the early Oligocene, forming an intraoceanic volcanic arc.

Ocean Drilling Program (ODP) Leg 125 was located in the Mariana and Izu-Bonin forearcs. An important goal of the leg was to investigate the origin and evolution of the forearc by drilling a series of holes that penetrated the subsurface sediments and basement of the Mariana and Izu-Bonin forearc basin as well as the serpentinite seamounts of the Mariana mid-forearc region and Izu-Bonin lower slope terrace. As part of meeting this goal, calcareous nannofossils were used to date the sedimentary and sediment-bearing volcanic sequences. This paper addresses the nannofossil stratigraphy of the Eocene-Miocene sediments. Nannofossils from the Pliocene to Quaternary interval were described by Ciampo (this volume).

Legs 59 and 60 of the Deep Sea Drilling Project (DSDP) are previous cruises that explored the study area and trench in the western Pacific Ocean in 1978. Samples from the two legs range in age from late middle or late Eocene to Pleistocene based on the calcareous nannofossils (Martini, 1980; Ellis, 1982).

During Leg 125, 15 holes at nine sites were drilled within the Mariana and Izu-Bonin forearcs. Six sites are located on or adjacent to serpentinite seamounts between the outer-arc high and trench. Four of these six sites are on Conical Seamount of the Mariana forearc; the other two are on Torishima Forearc Seamount of the Izu-Bonin

forearc. The remaining three sites (782, 785, and 786) are located along the eastern edge of the Izu-Bonin forearc basin (Fig. 1).

Eocene to Miocene sediments dated by calcareous nannofossils were found only in Holes 782A, 784A, 786A, and 786B (Fig. 2). More than 500 samples were examined by light microscopy, and 20 critical samples were selected for detailed study using scanning electron microscopy. Three hiatuses were detected as follows: within the lower Oligocene, between the upper Oligocene and middle Miocene, and between the middle and upper Miocene.

The standard low-latitude zonation of Okada and Bukry (1980) was used primarily in this paper, but not without some difficulties in certain intervals. As a result, the definitions of Subzones CP14a, CP14B, and CN1a were modified to facilitate their application in this area. The latitude, longitude, and water depth of the holes studied are indicated in Table 1.

METHODS

For each section, at least one smear slide from one sample was prepared directly from the raw sediment sample for examination at a magnification of 1560 \times . The distributions of coccoliths were recorded in the range charts. Samples from Hole 784A were also examined, although coccoliths are rare or barren there. The abundances of the individual nannofossil species from each smear slide were tabulated on range charts.

The format used to indicate relative abundance is as follows:

R = rare; 1 specimen per 101–1000 fields of view at 1560 \times
F = few; 1 specimen per 11–100 fields of view at 1560 \times
C = common; 1 specimen per 2–10 fields of view at 1560 \times
A = abundant; 1 or more specimens per field of view at 1560 \times .

A qualitative description of the preservation of nannofossils in each sample was recorded as follows:

G = good; no or little evidence of secondary alteration via etching and/or overgrowth; identification of species not impaired

¹ Fryer, P., Pearce, J. A., Stokking, L. B., et al., 1992. *Proc. ODP, Sci. Results*, 125: College Station, TX (Ocean Drilling Program).

² Department of Geology, Florida State University, Tallahassee, Florida 32306, U.S.A.

³ Present address: Department of Geology, China University of Geosciences, Beijing 100083, People's Republic of China.

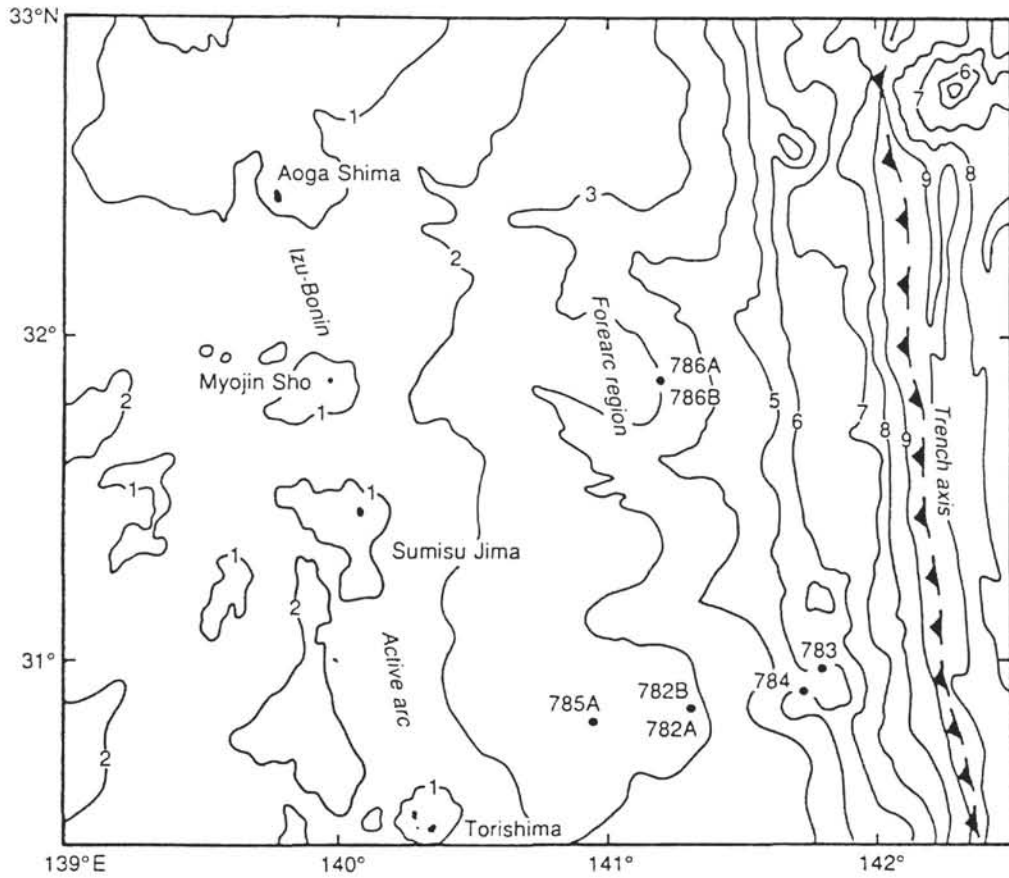
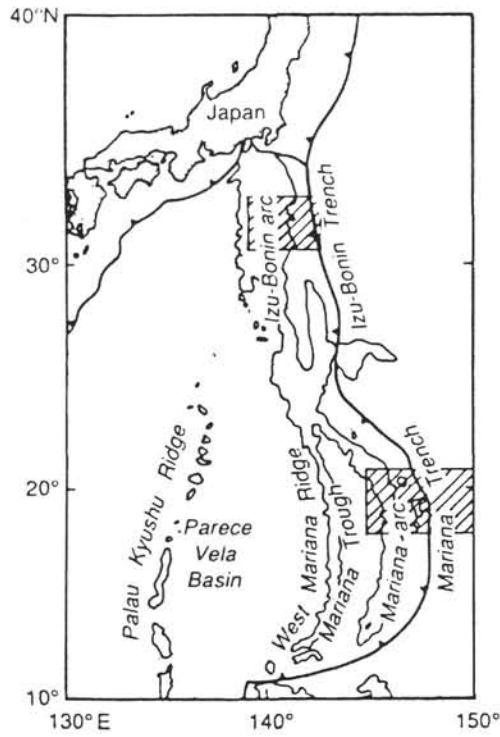


Figure 1. Location maps for ODP Leg 125 sites in the western Pacific Ocean.

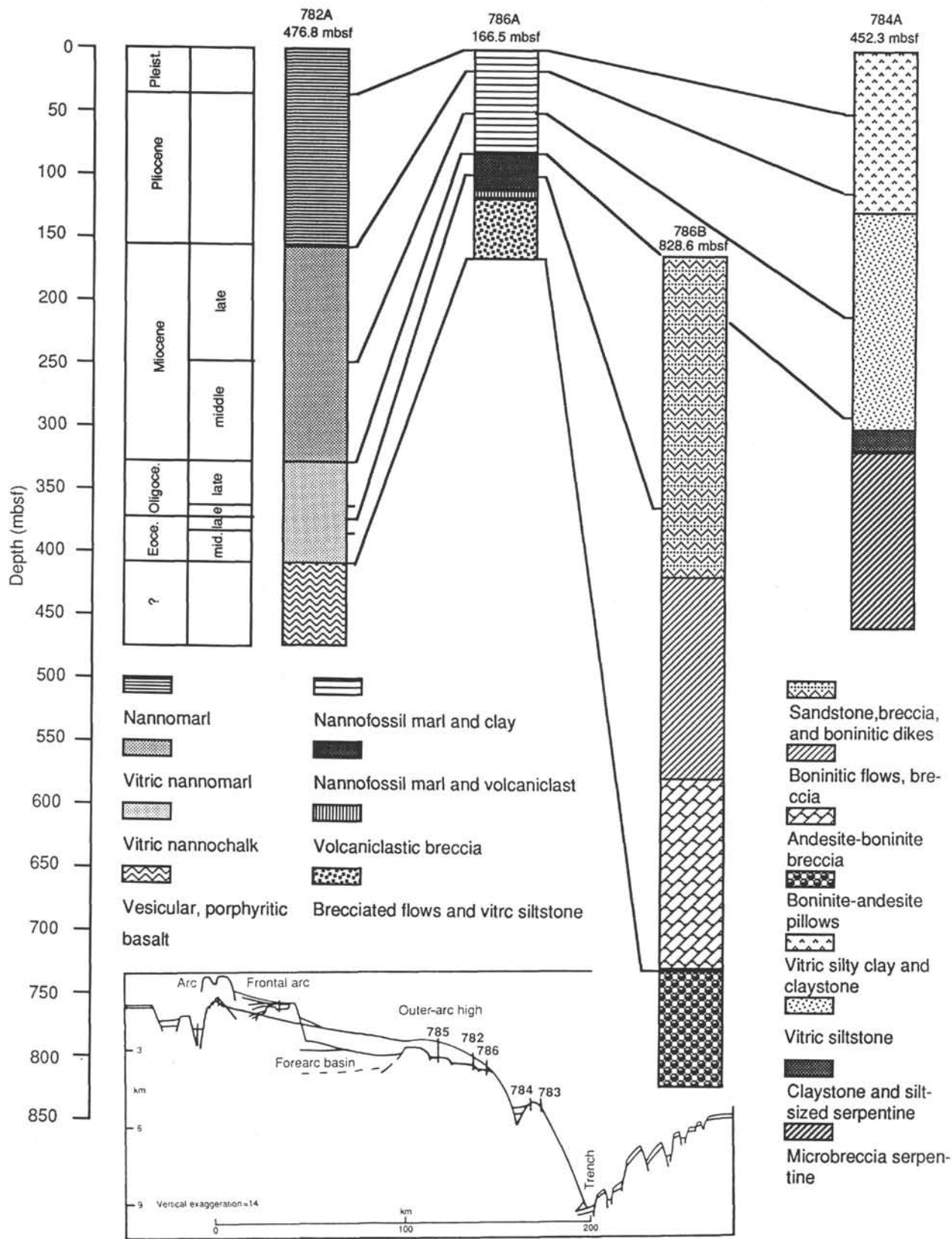


Figure 2. Stratigraphic correlation of Hole 782A with Holes 786A, 786B, and 784A.

Table 1. Latitude, longitude, and water depth of Holes 782A, 784A, 786A, and 786B.

Hole	Latitude (N)	Longitude (E)	Water Depth(m)
782A	30°51.66'	141°18.85'	2958.6
784A	30°54.49'	141°44.27'	4900.8
786A	31°52.48'	141°13.58'	3058.1
786B	31°52.45'	141°13.59'	3071.0

M = moderate; significant evidence of secondary alteration via etching and/or overgrowth; identification of species not impaired

P = poor; specimens with typically heavily overgrowth or severely etched; identification of some species significantly impaired.

CALCAREOUS NANNOFOSSIL BIOSTRATIGRAPHY AND ZONATION

The zonation scheme used for Cenozoic age determinations in this paper is the low-latitude zonation of Bukry (1973, 1975) and Okada and Bukry (1980). The absolute ages (geochronology) of the epochs and stages follow the scheme proposed by Berggren et al. (1985a, 1985b).

The Oligocene/Miocene boundary is placed in this paper between Subzones CN1a and CN1b (Bukry 1973, 1975; Okada and Bukry, 1980). Bukry (1975) correlated the end of the acme of *Cyclicargolithus floridanus abisectus* n. comb. with the Oligocene/Miocene boundary. In this paper, however, we found that common *Cyclicargolithus* cf. *abisectus* n. comb. extend up to Subzone CN5a and that no terminal Oligocene acme of this species can be discerned. The last occurrence (LO) of *Reticulofenestra bisecta* was found higher than the LO of *Sphenolithus ciperoensis*, which is used as the primary datum to define the Zone CP19/CN1 boundary. It is suggested that the LO of *R. bisecta* may best be used to mark the Oligocene/Miocene boundary and the top of CN1a.

The Eocene/Oligocene boundary in the study area is distinguished on the LOs of both *Discoaster barbadiensis* and *Discoaster saipanensis* in Holes 782A and 786A. In Hole 782A the disappearance of *Reticulofenestra reticulata* occurs at the same level.

Calcareous nannofossil species considered in this paper are listed in the Appendix, where they are arranged alphabetically by generic epithets. Bibliographic references for these taxa can be found in Loeblich and Tappan (1966, 1968, 1969, 1970a, 1970b, 1971, 1973), van Heck (1979a, 1979b, 1980a, 1980b, 1981a, 1981b, 1982a, 1982b, 1983), and Steinmetz (1985a, 1985b, 1986, 1987a, 1987b, 1988a, 1988b, 1989).

Nannofossil zones and subzones, oldest to youngest, are presented as follows (Table 2):

Coccolithus staurion Subzone (CP13c)

Definition. The base of the subzone cannot be defined in the study area because the marker species for CP13b, *Chiasmolithus gigas*, was not found. The top of the subzone is defined by the first occurrence (FO) of *Reticulofenestra umbilica* and *Discoaster bifax*.

Associated species. *Chiasmolithus expansus*, *Chiasmolithus grandis*, *Sphenolithus pseudoradians*, *Discoaster barbadiensis*, *Discoaster saipanensis*, *Coccolithus formosus*, and *Cyclicargolithus floridanus*.

Occurrence. Samples 125-782A-43X-CC to 125-782A-42X-2, 29–30 cm; Samples 125-786A-19X-CC to 125-786A-12X-1, 85 cm.

Age. Late middle Eocene.

Discoaster bifax Subzone (CP14a)

Definition (modified, this paper). The base of the subzone is defined by the FO of *Reticulofenestra umbilica* and the top by the LO of *Discoaster bifax* or the FO of *Reticulofenestra bisecta*.

Associated species. *Chiasmolithus expansus*, *Chiasmolithus grandis*, *Coccolithus formosus*, *Discoaster barbadiensis*, *Discoaster saipanensis*, *Sphenolithus pseudoradians*, and *Zygrhablithus bijugatus*.

Occurrence. Samples 125-782A-42X-1, 72–73 cm, to 125-782A-41X-CC; Samples 125-786A-12X-1, 40 cm, to 125-786A-11X-5, 65–66 cm.

Age. Late middle Eocene.

Discoaster saipanensis Subzone (CP14b)

Definition (modified, this paper). The base of the subzone is defined by the FO of *Reticulofenestra bisecta* or the LO of *Discoaster bifax*. The top is defined by the LO of *Chiasmolithus grandis* or the FO of *Chiasmolithus oamaruensis*.

Associated species. *Chiasmolithus expansus*, *Coccolithus formosus*, *Coronocyclus nitescens*, *Reticulofenestra reticulata*, *Discoaster barbadiensis*, *Discoaster saipanensis*, *Reticulofenestra umbilica*, and *Sphenolithus pseudoradians*.

Comment. Bukry (1973) used the LO of *Chiasmolithus solitus* as an alternate datum level for the top of this zone; however, this taxon was not observed in our sections. Instead, the FO of *Reticulofenestra bisecta* can be substituted as a marker species for the CP14a/CP14b boundary based on evidence from Holes 782A and 786A. This may be a more reliable datum than the FO of *C. solitus*, which appears to be a time-transgressive datum (W. Wei and S. W. Wise, Jr., unpubl. data).

Occurrence. Samples 125-782A-41X-7, 11–12 cm, to 125-782A-41X-4, 43–44 cm; Samples 125-786A-11X-4, 120 cm, to 125-786A-11X-3, 58–59 cm.

Age. Late middle Eocene.

Chiasmolithus oamaruensis Subzone (CP15a)

Definition. The base of the Subzone is defined by the LO of *Chiasmolithus grandis* or the FO of *Chiasmolithus oamaruensis*. The top of the subzone is defined by the FO of *Isthmolithus recurvus*.

Associated species. *Coccolithus formosus*, *Coronocyclus nitescens*, *Cyclicargolithus floridanus abisectus*, *Cyclicargolithus floridanus floridanus*, *Discoaster barbadiensis*, *Discoaster saipanensis*, *Reticulofenestra bisecta*, *Reticulofenestra reticulata*, *Reticulofenestra samodurovii*, *Reticulofenestra umbilica*, *Sphenolithus pseudoradians*, and *Zygrhablithus bijugatus*.

Comment. The subzone is determined only approximately, and is only 2 m thick in Hole 782A.

Occurrence. Samples 125-782A-41X-3, 60–61 cm, and 125-786A-11X-2, 70 cm.

Age. Late Eocene.

Isthmolithus recurvus Subzone (CP15b)

Definition. The base of the subzone is defined by the FO of *Isthmolithus recurvus* and the top by the LO of both *Discoaster barbadiensis* and *Discoaster saipanensis*.

Associated species. *Chiasmolithus oamaruensis*, *Coccolithus formosus*, *Coronocyclus nitescens*, *Helicosphaera compacta*, *Reticulofenestra bisecta*, *Reticulofenestra reticulata*, *Reticulofenestra umbilica*, and *Sphenolithus pseudoradians*.

Comment. The top of the subzone marks the nannofossil boundary between the Eocene and the Oligocene.

Table 2. Calcareous nannoplankton zonation scheme used for ODP Leg 125, and comparison with the zonation of Bukry (1973, 1975).

Age		Bukry zonation (1973,1975)		Zonation, this paper				
		Zone	Subzone	Zone	Subzone	Species datums		
Miocene	late	CN9 <i>Discoaster quinquerramus</i>	<i>Amaurolithus primus</i>	CN9 <i>Discoaster quinquerramus</i>	<i>Amaurolithus primus</i>	<i>Discoaster quinquerramus</i>		
			<i>Discoaster berggrenii</i>			<i>Discoaster berggrenii</i>	<i>Amaurolithus primus</i>	
	CN8 <i>Discoaster neohamatus</i>	<i>Discoaster neorectus</i>						
		<i>Discoaster bellus</i>						
	middle	CN7 <i>Discoaster hamatus</i>	<i>Catinaster calyculus</i>	CN7 <i>Discoaster hamatus</i>			<i>Discoaster hamatus</i>	
			<i>Helicosphaera carteri</i>				<i>Discoaster hamatus</i>	
		CN6 <i>Catinaster coalitus</i>		CN6 <i>Catinaster coalitus</i>			<i>Catinaster coalitus</i> <i>Discoaster kugleri</i>	
		CN5 <i>Discoaster exilis</i>	<i>Discoaster kugleri</i>	CN5 <i>Discoaster exilis</i>	<i>Discoaster kugleri</i>			<i>Discoaster kugleri</i>
			<i>Coccolithus miopelagicus</i>			<i>Coccolithus miopelagicus</i>	<i>Cyclicargolithus f. abisectus</i>	
	CN4 <i>Sphenolithus heteromorphus</i>		CN4 <i>Sphenolithus heteromorphus</i>				<i>Sphenolithus heteromorphus</i> <i>Calcidiscus macintyreii</i>	
early	CN3 <i>Helicosphaera ampliaperta</i>		CN3 <i>Helicosphaera ampliaperta</i>					
	CN2 <i>Sphenolithus belemnus</i>							
	CN1 <i>Triquetrorhabdulus carinatus</i>	<i>Discoaster druggii</i>						
<i>Discoaster deflandrei</i>								
Oligocene	late	CP19 <i>Sphenolithus ciproensis</i>	<i>Dictyococcites bisectus</i>	CP19 <i>Sphenolithus ciproensis</i>	<i>Reticulofenestra bisecta</i>	<i>Reticulofenestra bisecta</i>		
			<i>Cyclicargolithus floridanus</i>			<i>Cyclicargolithus f. floridanus</i>	<i>Sphenolithus ciproensis</i>	
	CP18 <i>Sphenolithus distentus</i>		CP17-CP18 <i>Sphenolithus distentus</i> - <i>Sphenolithus predistentus</i>				<i>Sphenolithus distentus</i>	
		CP17 <i>Sphenolithus predistentus</i>						
	CP16 <i>Helicosphaera reticulata</i>	<i>Reticulofenestra hillae</i>					<i>Coccolithus formosus</i> <i>Clausicoccus fenestratus</i>	
		<i>Coccolithus formosus</i>	CP16 <i>Helicosphaera reticulata</i>	<i>Coccolithus formosus</i>			<i>Discoaster saipanensis</i>	
<i>Coccolithus subdielichus</i>	<i>Clausicoccus fenestratus</i>	<i>Discoaster barbadiensis</i>						
Eocene	late	CP15 <i>Discoaster barbadiensis</i>	<i>Isthmolithus recurvus</i>	CP15 <i>Discoaster barbadiensis</i>	<i>Isthmolithus recurvus</i>	<i>Isthmolithus recurvus</i>		
			<i>Chiasmolithus oamaruensis</i>			<i>Chiasmolithus oamaruensis</i>	<i>Chiasmolithus grandis</i>	
	CP14 <i>Reticulofenestra umbilica</i>	<i>Discoaster saipanensis</i>	CP14 <i>Reticulofenestra umbilica</i>	<i>Discoaster saipanensis</i>			<i>Reticulofenestra bisecta</i> <i>Discoaster bifax</i>	
		<i>Discoaster bifax</i>			<i>Discoaster bifax</i>	<i>Reticulofenestra umbilica</i> <i>Discoaster bifax</i>		
middle	CP13 <i>Nannoletrina quadrata</i>	<i>Coccolithus staurion</i>	CP13		<i>Coccolithus staurion</i>			
		<i>Chiasmolithus gigas</i>						
		<i>Discoaster strictus</i>						

Occurrence. Samples 125-782A-41X-2, 111–112 cm, to 125-782A-40X-4, 16–17 cm; Samples 125-786A-11X-2, 62–64 cm, to 125-786A-11X-1, 8–10 cm.

Age. Late Eocene.

Clausicoccus fenestratus Subzone–*Coccolithus formosus* Subzone (CP16a-b)

Definition. The base of the *Clausicoccus fenestratus* Subzone is defined by the LO of both *Discoaster barbadiensis* and *Discoaster saipanensis*, and the top of the *Coccolithus formosus* Subzone is recognized by the LO of *Coccolithus formosus*.

Associated species. *Discoaster tani nodifer*, *Isthmolithus recurvus*, *Helicosphaera compacta*, *Reticulofenestra bisecta*, *Reticulofenestra umbilica*, *Sphenolithus predistentus*, and *Zygrhablithus bijugatus*.

Comment. According to the Bukry zonation (1975), the early Oligocene *Helicosphaera reticulata* Zone (CP16) was divided into the *Clausicoccus fenestratus* (= *Coccolithus subdisticus*) Subzone (CP16a), *Coccolithus formosus* Subzone (CP16b), and *Reticulofenestra hillae* Subzone (CP16c). In the study area, the marker events for the latter two subzones disappear simultaneously at the same level, which is overlain directly by the *Sphenolithus predistentus* and *Sphenolithus distentus* Zones (CP17–18). It is evident, therefore, that there is a hiatus between the *Coccolithus formosus* Subzone (CP16b) and *Sphenolithus predistentus* Zone (CP17), and that Zone CP16c is missing here. As well, no lower Oligocene acme of *Clausicoccus fenestratus* was recognized at any Leg 125 site.

Occurrence. Samples 125-782A-40X-3, 16–17 cm, to 125-782A-39X-CC; Samples 125-786A-10X-CC to 125-786A-10X-4, 14–15 cm.

Age. Early early Oligocene.

Sphenolithus predistentus–*Sphenolithus distentus* Zones (CP17–18)

Definition. The base of the zones is defined by the FO of *Sphenolithus distentus* and the top by the FO of *Sphenolithus ciperoensis*.

Associated species. *Cyclicargolithus abisectus*, *Cyclicargolithus floridanus*, *Discoaster deflandrei*, *Discoaster tani nodifer*, *Helicosphaera compacta*, *Reticulofenestra bisecta*, *Sphenolithus predistentus*, and *Sphenolithus pseudoradians*.

Comment. The interval corresponding to Bukry's *Sphenolithus predistentus* (CP17) and *Sphenolithus distentus* Zone (CP18) can be recognized in Hole 782A. In Hole 786A, however, *Sphenolithus distentus* extends down to the lower Oligocene Zone CP16, where it coexists with *Coccolithus formosus* and *Reticulofenestra umbilica*. This was also true for Leg 115 in the Indian Ocean (Backman et al., 1990). Therefore, the base of the zone is only tentatively delineated and a more reliable marker species than *Sphenolithus distentus* needs to be assigned in future studies.

Comment. The combined zones are found only in Hole 782A (not in Hole 786A).

Occurrence. Samples 125-782A-39X-CC, 26–27 cm, to 125-782A-39X-1, 111 cm.

Age. Late early Oligocene.

Cyclicargolithus floridanus floridanus Subzone (CP19a)

Definition. The base is defined by the FO of *Sphenolithus ciperoensis* and the top by the LO of *Sphenolithus distentus*.

Associated species. *Cyclicargolithus floridanus abisectus* n. comb., *Cyclicargolithus floridanus floridanus*, *Dictyococcites daviesii*, *Discoaster deflandrei*, *Discoaster delicatus*, *Sphenolithus predistentus*, *Triquetrorhabdulus milowii*, and *Zygrhablithus bijugatus*.

Comment. The top of the subzone is recognized by the LO of *Sphenolithus predistentus*.

Occurrence. Samples 125-782A-39X-1, 28–29 cm, to 125-782A-37X-1, 61–62 cm; Sample 125-786A-10X-3, 14–15 cm.

Age. Early late Oligocene.

Reticulofenestra bisecta Subzone (CP19b)

Definition. The base of the subzone is defined by the LO of *Sphenolithus distentus* and the top by the LO of *Sphenolithus ciperoensis*.

Associated species. *Cyclicargolithus floridanus abisectus* n. comb., *Cyclicargolithus floridanus floridanus*, *Discoaster deflandrei*, *Discoaster delicatus*, *Reticulofenestra umbilica*, *Sphenolithus conicus*, *Triquetrorhabdulus carinatus*, and *Triquetrorhabdulus milowii*.

Comment. The top of the subzone was defined in part by the LO of *Reticulofenestra bisecta* based on Bukry (1975) and Okada and Bukry (1980), but the species ranges up into Subzone CN1a in the study area.

Occurrence. Samples 125-782A-36X-CC to 125-782A-35X-7, 25–26 cm; Samples 125-786A-10X-2, 14–15 cm, to 125-786A-9X-6, 14–15 cm.

Age. Late late Oligocene.

Cyclicargolithus floridanus abisectus Subzone (CN1a)

Definition (modified, this paper). The base of the subzone is defined by the LO of *Sphenolithus ciperoensis*, and the top by the LO of *Reticulofenestra bisecta*.

Associated species. *Cyclicargolithus floridanus abisectus* n. comb., *Cyclicargolithus floridanus*, *Discoaster deflandrei*, *Reticulofenestra bisecta*, and *Triquetrorhabdulus carinatus*.

Comment. The top of the subzone approximates the Oligocene/Miocene boundary (Bukry, 1975). Note that the distribution of *Cyclicargolithus f. abisectus* n. comb. extends up through Subzone CN5a (middle Miocene) in the study area. In addition, an upper Oligocene termination of an acme of this taxon was not observed at any site of Leg 125. The subzone as originally defined by Bukry (1973), therefore, could not be used here. The distribution of *Reticulofenestra bisecta*, the LO of which was taken by Bukry to define the top of CP19b, extends up beyond the LO of *Sphenolithus ciperoensis* both at our sites and elsewhere (Biolzi, 1985; Wei and Wise, 1989). As such, this event can be used to mark the top of Subzone CN1a in lieu of the LO of the acme of *C. f. abisectus* n. comb. We believe this is the best choice of the available nannofossil datums to approximate the Oligocene/Miocene boundary (bottom of Chron C6B). These results coincide with those of Berggren et al. (1985a), in which the LO of *Reticulofenestra bisecta* is 23.7 Ma, corresponding to the Oligocene/Miocene boundary. In addition, Wei and Wise (1989, fig. 23) found this to be a reliable datum across a number of mid-latitude sites in the North and South Atlantic that lie at a latitude similar to that of our study area.

Occurrence. Samples 125-782A-35X-6, 129–130 cm, to 125-782A-35X-6, 4–5 cm; Samples 125-786A-9X-5, 80 cm, to 125-786A-9X-5, 62–63 cm.

Age. Latest Oligocene.

Helicosphaera ampliapertura Zone (CN3)

Definition. The base of the zone is defined by the FO of *Sphenolithus heteromorphus* and the top by the FO of *Calcidiscus macintyreii*.

Associated species. *Coronocyclus nitescens*, *Cyclicargolithus floridanus floridanus*, *Discoaster deflandrei*, and *Reticulofenestra pseudumbilica*. *Helicosphaera ampliapertura* was not observed at our sites.

Comment. According to the Bukry zonation, the base of the CN3 Zone is recognized by the LO of *Sphenolithus belemnus*, and the top is defined by the LO of *Helicosphaera ampliapertura* (Bukry, 1973) or the FO of *Calcidiscus macintyreii* (Bukry, 1975). In the study area, however, *Sphenolithus belemnus* and *Helicosphaera ampliapertura* were not observed, and *Calcidiscus macintyreii* was found right above the LO of *Reticulofenestra bisecta* in Hole 782A. These facts indicate

that a hiatus is present between the late Oligocene and the middle Miocene and that Zones/Subzones CN1b, CN1c, and CN2 and part of CN3 are missing here.

Occurrence. Samples 125-782A-35X-5, 120–121 cm, to 125-782A-35X-3, 60–61 cm. Samples 125-786A-8X-1, 35–36 cm, to 125-786A-9X-5, 57–58 cm, may belong to this zone or the zone above (see subsequent comments).

Age. Late early Miocene.

Sphenolithus heteromorphus Zone (CN4)

Definition. The base of the zone is defined by the FO of *Calcidiscus macintyre* (782A) and the top of the zone by the LO of *Sphenolithus heteromorphus*.

Associated species. *Cyclicargolithus floridanus abisectus* n. comb., *Cyclicargolithus floridanus floridanus*, *Discoaster deflandrei*, *Discoaster variabilis*, and *Reticulofenestra pseudoumbilica*.

Comment. In Hole 786A, the base of Zone CN4 cannot be recognized because *C. macintyre* is absent throughout this part of the section (including in the overlying Zone CN5), probably due to problems of preservation. As noted previously, the marker species, *Helicosphaera ampliaperta*, is also absent.

Occurrence. Samples 125-782A-35X-2, 83–84 cm, to 125-782A-33X-7, 11–16 cm; Samples 125-786A-9X-5, 57–58 cm, to 125-786A-8X-1, 35–36 cm, may belong to this zone or to Zone CN3.

Age. Early middle Miocene.

Coccolithus miopelagicus Subzone (CN5a)

Definition. The base of the subzone is defined by the LO of *Sphenolithus heteromorphus*, and the top of the subzone is defined by the FO of *Discoaster kugleri* or by the LO of *Cyclicargolithus floridanus*.

Associated species. *Calcidiscus macintyre*, *Coronocyclus nitescens*, *Discoaster variabilis*, *Reticulofenestra pseudoumbilica*, and *Cyclicargolithus floridanus*.

Comment. The subzone was found only in Hole 782A, where both subspecies of *Cyclicargolithus floridanus* were present. Martini (1980) reported *Cyclicargolithus floridanus abisectus* n. comb. as rare to few in the lower part of this interval (his Zone NN6) and common in the zone below (his NN5).

Occurrence. Samples 125-782A-33X-6, 78–83 cm, to 125-782A-30X-1, 54–55 cm.

Age. Middle middle Miocene.

Discoaster kugleri Subzone (CN5b)

Definition. The base of the subzone is defined by the FO of *Discoaster kugleri* or, alternatively, by the LO of *Cyclicargolithus floridanus*, and the top is defined by the FO of *Catinaster coalitus* (alternatively, the LO of *Discoaster kugleri* could be used to approximate this datum).

Associated species. *Calcidiscus macintyre*, *Coronocyclus nitescens*, *Discoaster exilis*, and *Reticulofenestra pseudoumbilica*.

Occurrence. Samples 125-782A-29X-CC to 125-782A-27X-2, 108–109 cm; Samples 125-786A-7X-CC to 125-786A-6X-3, 51–52 cm.

Age. Middle middle Miocene.

Catinaster coalitus Zone (CN6)

Definition. The base of the zone is defined by the FO of *Catinaster coalitus* and the top by the FO of *Discoaster hamatus*.

Associated species. *Catinaster calyculus*, *Discoaster brouweri*, *Discoaster calcaris*, *Discoaster exilis*, *Discoaster variabilis*, and *Reticulofenestra pseudoumbilica*.

Comment. Zones CN6 and CN7 cannot be separated at Hole 786A because of the absence of *Discoaster hamatus*.

Occurrence. Samples 125-782A-27X-1, 109–110 cm, to 125-782A-26X-6, 92–93 cm.

Age. Middle middle Miocene.

Discoaster hamatus Zone (CN7)

Definition. The base of the zone is defined by the FO of *Discoaster hamatus* and the top by the LO of *Discoaster hamatus*.

Associated species. *Catinaster calyculus*, *Catinaster mexicanus*, *Discoaster brouweri*, *Discoaster calcaris*, *Discoaster exilis*, *Discoaster variabilis*, and *Reticulofenestra pseudoumbilica*.

Comment. The *Discoaster hamatus* Zone was divided into two subzones by the FO of *Catinaster calyculus* by Okada and Bukry (1980). *Catinaster calyculus*, however, appears prior to the FO of *Discoaster hamatus* at our sites; Subzones *Helicosphaera carteri* (CN7a) and *Catinaster calyculus* (CN7b), therefore, cannot be recognized in this paper. Martini (1980, tables 2 and 3) recorded the same succession for *C. calyculus* and *D. hamatus* at DSDP Sites 448 and 450 in this region and indicated that this is the correct order of appearance for these two taxa. This is opposite the order of succession reported by Bukry (1973, 1975). Relying in part on rotary-cored core-catcher samples, Ellis (1982) found the first uphole occurrence of *C. calyculus* below *D. hamatus* at Site 458 but above it at Site 459. He opted to follow Bukry's interpretation of the succession.

Occurrence. Samples 125-782A-20X-5, 92–93 cm, to 125-782A-26X-3, 92–93 cm.

Age. Late middle Miocene.

Discoaster berggrenii Subzone (CN9a)

Definition. The base of the subzone is defined by the FO of *Discoaster berggrenii* and the top by the FO of *Amaurolithus primus*.

Associated species. *Amaurolithus tricoraniculatus*, *Calcidiscus leptoporus*, *Discoaster berggrenii*, *Discoaster quinqueramus*, *Discoaster surculus*, *Discoaster variabilis*, *Reticulofenestra pseudoumbilica*, *Sphenolithus abies*, and *Triquetrorhabdulus rugosus*.

Comment. A hiatus is present between the *Discoaster hamatus* Zone (CN7) and the *Discoaster berggrenii* Subzone (CN9a) because *Discoaster neorectus* is absent here and the FO of *Discoaster quinqueramus* (Sample 125-782A-26X-3, 92–93 cm) follows directly on the LO of *Catinaster coalitus* and *Catinaster calyculus* (Sample 125-782A-26X-4, 92–93 cm).

Occurrence. Samples 125-782A-26X-2, 92–93 cm, to 125-782A-20X-CC; Samples 125-786A-5X-CC to 125-786A-5X-1, 131–132 cm.

Age. Late late Miocene.

Amaurolithus primus Subzone (CN9b)

Definition. The base of the subzone is defined by the FO of *Amaurolithus primus* and the top by the FO of *Ceratolithus acutus*.

Associated species. *Amaurolithus delicatus*, *Amaurolithus tricoraniculatus*, *Calcidiscus leptoporus*, *Calcidiscus macintyre*, *Discoaster berggrenii*, *Discoaster brouweri*, *Discoaster surculus*, *Discoaster variabilis*, *Helicosphaera kamptneri*, *Reticulofenestra pseudoumbilica*, *Sphenolithus abies*, and *Triquetrorhabdulus rugosus*.

Comment. The top of Subzone CN9b marks the Miocene/Pliocene boundary. The overlying subzone (CN10a) is a "gap" zone that was not observed in our holes. Temporarily, CN10a is a short subzone that is not observed in many oceanic sections, particularly those which are not expanded sections. Gartner et al. (1983) suggested that the zone may not even exist except where environmental control and general sparseness of the index taxa serve to open up the "gap" between the defining datums (such as in the Mediterranean Basin). If this short subzone does exist in open-ocean environments, close sampling and good core recovery would be necessary to allow its detection, and any reworking of the basal marker, *D. quinqueramus*, would tend to

obscure it. Hiatuses at the Miocene/Pliocene boundary are also not uncommon in the geologic record. For these various reasons, Subzone CN10a is not commonly reported in the literature, nor was it detected in our holes. Instead, Subzone CN10b was reported in the cores taken immediately above those of the sections we studied (see chapters for Sites 782 and 786, Fryer, Pearce, Stokking, et al., 1990; also Ciampo, this volume).

Occurrence. Samples 125-782A-20X-1, 35–36 cm, to 125-782A-17X-1, 92–93 cm; Samples 125-786A-4X-CC to 125-786A-4X-1, 96–97 cm.

Age. Late late Miocene.

SUMMARY OF NANNOFOSSIL STRATIGRAPHY

In this study area, Eocene to Miocene calcareous nannofossils were found only in Holes 782A, 784A, 786A, and 786B. The background information and detailed description of cores from the following drill sites are given in the appropriate site chapters of Volume 125 of the *Proceedings of the Ocean Drilling Program, Initial Reports* (Fryer, Pearce, Stokking, et al., 1990).

Hole 782A

Hole 782A is located on the eastern margin of the Izu-Bonin forearc, about halfway between the active volcanic arc and the trench. The sediments are 409.2 m thick, ranging from Pleistocene to middle Eocene in age, and have been divided into three lithostratigraphic subunits overlying basal angular to subrounded clasts of intermediate acid lava.

Three unconformities were identified from the succession: the first is located between the middle and upper Miocene, a second between the upper Oligocene and middle Miocene; and the third within the lower Oligocene (Table 3, microfiche in back pocket).

Miocene

Common to abundant, moderately preserved Miocene nannofossils are present from Samples 125-782A-17X-1, 92–93 cm, to 125-782A-35X-5, 120–121 cm.

Within the upper Miocene interval, the top of Subzone CN9b is marked by the LO of *Discoaster quinqueramus* together with *Discoaster berggrenii* and *Triquetrorhabdulus rugosus* in Sample 125-782A-17X-1, 92–93 cm. The FO of *Ceratolithus acutus*, which marks the base of the early Pliocene Subzone CN10b, occurs in Sample 125-782A-16X-CC. Therefore, the Miocene/Pliocene boundary is placed within the interval between Cores 125-782A-17X and 125-782A-16X (Fryer, Pearce, Stokking, et al., 1990; see also Ciampo, this volume, for the nannofossil stratigraphy of the Pliocene). As discussed in the previous section, there can be several reasons why the short Subzone CN10a was not detected in this hole. Because the boundary falls between two cores recovered with the extended core barrel (XCB), it may have not been sampled as there is always some sediment loss between cores. Alternatively, this zone may not exist everywhere (Gartner et al., 1983) or there may be a minor hiatus at this site. The latter possibility may be likely here because *D. berggrenii* and *D. quinqueramus* co-occur essentially to the top of Section 125-782A-16X-CC. In a complete section, *D. quinqueramus* would be expected to extend a bit higher than *D. berggrenii* (Perch-Nielsen, 1985, fig. 7). The fact that the upper contact of Subzone CN9b was not captured within a core, however, does not allow us to state more specifically why the lowermost Pliocene Subzone CN10a was not detected at this site.

The FO of *Amaurolithus primus*, defining the boundary between Subzone CN9a and Subzone CN9b, is recognized in Sample 125-782A-

20X-1, 35–36 cm. The base of Subzone CN9a is placed at Sample 125-782A-26X-2, 92–93 cm, based on the FO of *Discoaster quinqueramus*. The Subzone CN9a/CN9b boundary is located within the interval from Samples 125-782A-20X-1, 35–36 cm, to 125-782A-20X-CC.

The marker species of Subzone CN8b, *Discoaster neorectus* and *Discoaster loeblichii*, are missing from this section, and Zone CN9 succeeds the LO of *Catinaster coalitus*, *Catinaster calyculus*, and *Discoaster hamatus*. It is, therefore, evident that there is a hiatus between Zones CN7 and CN9 within the interval from Samples 125-782A-26X-3, 92–93 cm, to 125-782A-26X-2, 92–93 cm, and it is dated as lasting 0.7 m.y. by the time scale of Berggren et al. (1985b).

The base of Zone CN7 is defined by the FO of *Discoaster hamatus* from Sample 125-782A-26-5X, 92–93 cm. Subzones CN7a and CN7b cannot be separated in this paper because the FO of *Catinaster calyculus* (Sample 125-782A-26X-6, 92–93 cm) occurs prior to that of *Discoaster hamatus* in this hole.

The FO of *Catinaster coalitus*, which defines the Zone CN5/CN6 boundary, is in Sample 125-782A-27X-1, 109–110 cm. It is important to note that the LO of *Catinaster coalitus* from Sample 125-782A-26X-4, 92–93 cm, coincides with the disappearance of *Catinaster calyculus*. This confirms the hiatus between Zones CN7 and CN9.

Subzones CN7a and CN7b cannot be separated in this paper because *Discoaster hamatus* is rare in Hole 782A and absent in Hole 786A, and the FO of *Catinaster calyculus* occurs below that of *Discoaster hamatus*.

The middle middle Miocene *Discoaster exilis* Zone (CN5) is assigned from Samples 125-782A-33X-6, 78–83 cm, to 125-782A-27X-2, 108–109 cm, based on the LO of *Sphenolithus heteromorphus* and the LO of *Discoaster kugleri*. The CN5/CN4 boundary is within the interval from Samples 125-782A-33X-6, 78–83 cm, to 125-782A-33X-7, 11–16 cm, whereas the bottom of the *Discoaster kugleri* Subzone (CN5b) is indicated by the FO of *Discoaster kugleri* in Sample 125-782A-29X-CC. The LO of *Cyclicargolithus f. floridanus*, a secondary marker for the base of Subzone CN5b, was found in Sample 125-782A-29X-6, 134–135 cm. The LO of *C. f. abisectus* n. comb. occurs at the same level.

The early middle Miocene *Sphenolithus heteromorphus* Zone (CN4) is placed within the interval from Samples 125-782A-35X-2, 83–84 cm, to 125-782A-33X-7, 11–16 cm, by the occurrence of *Sphenolithus heteromorphus* together with *Discoaster deflandrei*, *Discoaster variabilis*, *Cyclicargolithus f. abisectus* n. comb., and the absence of *Helicosphaera ampliaptera*.

The interval from Samples 125-782A-35X-5, 120–121 cm, to 125-782A-35X-3, 60–61 cm, is assigned to the upper part of the CN3 Zone based on the FO of *Calcidiscus macintyreii* (Sample 125-782A-35X-2, 83–84 cm) at the top of that zone.

Reticulofenestra bisecta was found in Sample 125-782A-35X-6, 4–5 cm, just below the *Helicosphaera ampliaptera* Zone. In addition, the marker species for Zones CN1 and CN2 and lower part of CN3 (*Sphenolithus belemnoides*, *Discoaster druggii*, and *Helicosphaera ampliaptera* Zones) were not found here. These facts indicate that Sample 125-782A-35X-6, 4–5 cm, and the sediments immediately below are late Oligocene in age, and that a hiatus must be present between the middle Miocene and upper Oligocene within the interval from Samples 125-782A-35X-5, 120–121 cm, to 125-782A-35X-6, 4–5 cm. This hiatus would span more than 7.5 m.y. by the time scale of Berggren et al. (1985a).

According to the lithostratigraphic data of Hole 782A, an unconformity is also present from Sections 125-782A-35X-5, 145–150 cm, to 125-782A-35X-6, 0–8 cm. This boundary is marked by a black, 5-cm-thick layer of 1-mm to 2-cm manganese nodules underlain by a reddish brown clay and overlain by a 2-cm-thick yellowish brown, finely laminated siltstone (see “Lithostratigraphy” section for Hole 782A, Fryer, Pearce, Stokking, et al., 1990).

Table 3. Distribution of calcareous nannofossil species, Hole 782A.

Lithologic unit	Age	Zone (Bukry, 1973, 1975)	Core, section, interval (cm)	Abundance	Preservation	<i>Amaurolithus delicatus</i>	<i>Amaurolithus primus</i>	<i>Amaurolithus tricorniculatus</i>	<i>Blackites spinosus</i>	<i>Calcidiscus leptoporus</i>	<i>Calcidiscus macintyreii</i>	<i>Campylophoera dela</i>	<i>Catinaster calyculus</i>	<i>Catinaster coalitus</i>	
IC		<i>Amaurolithus primus</i> Subzone (CN9b)	17X-1, 92-93	A	M	•	•	•	•	•	C	•	•	•	
			17X-2, 92-93	C	M	•	•	•	•	•	•	F	•	•	•
			17X-3, 92-93	C	M	R	•	•	•	•	•	F	•	•	•
			17X-4, 92-93	C	M	•	•	•	•	•	•	C	•	•	•
			17X-5, 92-93	A	M	R	•	•	•	•	•	C	•	•	•
			17X-CC	A	M	R	R	•	•	•	•	C	•	•	•
			18X-1, 26-27	A	M	•	R	•	•	•	•	C	•	•	•
			18X-1, 130-131	A	M	•	•	•	•	•	•	C	•	•	•
			18X-2, 26-27	C	M	R	R	•	•	•	•	C	•	•	•
			18X-CC	A	M	R	•	R	•	•	•	C	•	•	•
			19X-1, 33-34	A	G	R	•	•	•	•	F	F	•	•	•
			19X-3, 46-47	A	M	R	•	•	•	•	F	•	•	•	•
			19X-3, 130-131	A	M	R	•	R	•	•	C	F	•	•	•
			19X-CC	A	M	R	•	•	•	•	C	•	•	•	•
			20X-1, 35-36	A	M	R	R	•	•	•	C	•	•	•	•
			20X-CC	A	G	R	•	•	•	•	C	•	•	•	•
			21X-1, 118-119	C	M	•	•	•	•	•	C	•	•	•	•
			21X-2, 118-119	A	G	R	•	•	•	•	C	F	•	•	•
			21X-3, 118-119	A	G	R	•	•	•	•	A	•	•	•	•
			21X-4, 110-111	A	M	•	•	•	•	•	C	•	•	•	•
			21X-5, 71-72	C	M	•	•	•	•	•	C	F	•	•	•
			21X-CC	A	G	•	•	•	•	•	R	•	•	•	•
			22X-1, 49-50	A	M	•	•	•	•	•	C	•	•	•	•
			22X-2, 28-29	A	M	•	•	•	•	•	•	R	•	•	•
			22X-CC	A	M	•	•	•	•	•	C	R	•	•	•
			23X-1, 67-68	C	M	•	•	•	•	•	F	•	•	•	•
			23X-2, 67-68	A	M	•	•	•	•	•	•	•	•	•	•
			23X-3, 68-69	A	M	•	•	•	•	•	R	R	•	•	•
			23X-4, 57-58	A	M	•	•	•	•	•	C	•	•	•	•
			23X-5, 77-78	A	M	•	•	•	•	•	F	•	•	•	•
			23X-6, 79-80	A	M	•	•	•	•	•	F	•	•	•	•
			23X-7, 17-18	A	G	•	•	•	•	•	F	•	•	•	•
			23X-CC	A	M	•	•	•	•	•	F	•	•	•	•
			24X-1, 40-41	A	G	•	•	•	•	•	F	•	•	•	•
			24X-2, 10-11	A	M	•	•	•	•	•	F	•	•	•	•
			24X-CC	A	G	•	•	•	•	•	C	R	•	•	•
			25X-1, 67-68	C	M	•	•	•	•	•	C	•	•	•	•
			25X-2, 98-99	C	M	•	•	•	•	•	F	•	•	•	•
			25X-3, 109-110	A	M	•	•	•	•	•	•	•	•	•	•
			25X-4, 117-118	A	M	•	•	•	•	•	C	•	•	•	•
	25X-5, 70-71	A	M	•	•	•	•	•	•	•	•	•	•		
	25X-6, 128-129	A	M	•	•	•	•	•	•	•	•	•	•		
	25X-7, 6-7	C	M	•	•	•	•	•	•	•	•	•	•		
	25X-CC	C	M	•	•	•	•	•	•	R	•	•	•		
	26X-1, 92-93	A	M	•	•	•	•	•	•	R	•	•	•		
	26X-2, 92-93	C	M	•	•	•	•	•	F	•	•	•	•		
	26X-3, 92-93	A	G	•	•	•	•	•	F	•	•	•	•		
	26X-4, 92-93	A	M	•	•	•	•	•	•	R	•	C	F		
	26X-5, 92-93	A	G	•	•	•	•	•	•	•	•	R	F		
	26X-6, 92-93	A	G	•	•	•	•	•	F	•	•	F	F		
	26X-CC	A	G	•	•	•	•	•	F	R	•	•	C		
	27X-1, 109-110	A	G	•	•	•	•	•	F	•	•	•	F		
	27X-2, 108-109	A	M	•	•	•	•	•	F	R	•	•	•		
	27X-3, 9-10	A	G	•	•	•	•	•	•	F	•	•	•		
	27X-CC	A	M	•	•	•	•	•	•	R	•	•	•		
	28X-1, 42-43	A	M	•	•	•	•	•	R	C	•	•	•		
	28X-2, 105-106	A	M	•	•	•	•	•	F	R	•	•	•		
	28X-3, 39-40	A	M	•	•	•	•	•	F	R	•	•	•		
	28X-4, 103-104	C	M	•	•	•	•	•	F	•	•	•	•		
	28X-5, 37-38	C	G	•	•	•	•	•	•	F	•	•	•		
	28X-6, 127-128	C	M	•	•	•	•	•	•	•	•	•	•		
	28X-CC	C	M	•	•	•	•	•	•	R	•	•	•		
	29X-1, 103-104	A	M	•	•	•	•	•	•	R	•	•	•		
	29X-2, 63-64	A	M	•	•	•	•	•	•	•	F	•	•		
	29X-3, 96-97	C	M	•	•	•	•	•	•	F	F	•	•		
	29X-3, 97-98	C	M	•	•	•	•	•	•	R	R	•	•		
	29X-4, 48-49	A	M	•	•	•	•	•	•	R	R	•	•		
	29X-5, 82-83	A	M	•	•	•	•	•	•	•	R	•	•		
	29X-6, 134-135	A	M	•	•	•	•	•	R	R	•	•	•		
	29X-CC	A	M	•	•	•	•	•	F	F	•	•	•		

Entirety of Table 3 is on microfiche in back pocket.

Oligocene

The interval from Samples 125-782A-35X-6, 4–5 cm, to 125-782A-40X-3, 16–17 cm, yielded abundant Oligocene nannofossil assemblages. The status of preservation varies from good to moderate, and is generally better than that of the Miocene.

The uppermost Oligocene *Cyclicargolithus f. abisectus* Subzone (CN1a) is defined herein by the LO of *Reticulofenestra bisecta* at the top of the subzone (Sample 125-782A-35X-6, 4–5 cm) and at its base by the LO of *Sphenolithus ciperoensis* (Sample 125-782A-35X-6, 129–130 cm). It is only 125 cm thick.

The LO of the acme of *Cyclicargolithus f. abisectus* n. comb. has been used to mark the Subzone CN1a/CN1b boundary according to Bukry's (1973, 1975) zonation. In the study area, however, common *Cyclicargolithus f. abisectus* n. comb. extend higher into the middle Miocene (to Sample 125-782A-29X-6, 134–135 cm; base of Subzone CN5b). Likewise, the LO of *Reticulofenestra bisecta*, traditionally used to mark the CP19b/CP19a boundary in Bukry's zonation, extends above the LO of *Sphenolithus ciperoensis*. Thus, the LOs of these two species are not necessarily synchronous as demonstrated by Wei and Wise (1989), and in Hole 782A the LO of *Reticulofenestra bisecta* is the best approximation of the Oligocene/Miocene boundary. This taxon is also used to approximate this boundary in middle to high (but not extreme high) latitudes where sphenoliths are sparse or absent (see discussion by Wei and Wise, 1989). Zone CP19 is defined by the occurrence of *Sphenolithus ciperoensis* from Samples 125-782A-39X-1, 28–29 cm, to 125-782A-35X-7, 25–26 cm. It can be divided into two subzones by the LO of *Sphenolithus distentus*, which marks the Subzone CP19a/CP19b boundary within the interval from Samples 125-782A-37X-1, 62–63 cm, to 125-782A-36X-CC.

The late early Oligocene Zone CP17-18 is defined by the FO of *Sphenolithus distentus* at the base in Sample 125-782A-39X-CC, 26–27 cm, and the FO of *Sphenolithus ciperoensis* at the top in Sample 125-782A-39X-1, 111 cm.

The interval from Samples 125-782A-40X-3, 16–17 cm, to 125-782A-29X-CC is assigned to the lowermost Oligocene by the presence of *Coccolithus formosus* and *Clausicoccus fenestratus* together with *Isthmolithus recurvus*, *Reticulofenestra bisecta*, *Reticulofenestra umbilica*, and *Sphenolithus predistentus* and the absence of *Discoaster barbadiensis* and *Discoaster saipanensis*. *Coccolithus formosus*, *Clausicoccus fenestratus*, and *Reticulofenestra umbilica* disappear simultaneously in Sample 125-782A-39X-CC, which is right below Zone CP17-18. It is therefore obvious that Subzone CP16c is missing; the hiatus within the interval from Samples 125-782A-39X-CC, 26–27 cm, to 125-782A-39X-CC can be dated as more than 0.6 m.y. by the time scale of Berggren et al. (1985a).

Eocene

The interval from Samples 125-782A-40X-4, 16–17 cm, to 125-782A-41X-3, 60–61 cm, yields the upper Eocene Zone CP15. The common species in this zone include *Discoaster barbadiensis*, *Discoaster saipanensis*, *Chiasmolithus oamaruensis*, *Isthmolithus recurvus*, and *Reticulofenestra reticulata*. Zone CP15 can be divided into the *Chiasmolithus oamaruensis* Subzone from Samples 125-782A-40X-4, 16–17 cm, to 125-782A-41X-2, 111–112 cm, and the *Isthmolithus recurvus* Subzone in Sample 125-782A-41X-3, 60–61 cm.

Zone CP14 is recognized by the FOs of *Reticulofenestra umbilica* and *Discoaster bifax* at the base (Sample 125-782A-42X-1, 72–73 cm) and by the LO of *Chiasmolithus grandis* or the FO of *Chiasmolithus oamaruensis* at the top (Sample 125-782A-41X-4, 43–44 cm). The *Reticulofenestra umbilica* Zone (CP14) can be divided into two subzones based on the LO of *Discoaster bifax* or the FO of *Reticulofenestra bisecta*. The Subzone CP14a/CP14b boundary is located within the interval from Samples 125-782A-41X-7, 11–12 cm, to 125-782A-41X-CC.

The boundary between Zone CP14 and Zone CP13 is distinct, based on the presence and absence of *Reticulofenestra umbilica*

within the interval from Samples 125-782A-42X-1, 72–73 cm, to 125-782A-42X-2, 29–30 cm, respectively. The *Coccolithus staurion* (CP13c) Subzone is present, based on the absence of *Chiasmolithus gigas*.

The Eocene nannofossils are common to abundant, and moderate to well preserved. The late middle to late Eocene age sediments here directly overlie the volcanic basement, and their base is dated as 44.4–47.0 Ma according to the Berggren et al. (1985a) time scale.

Hole 784A

Hole 784A is located approximately 7 km southwest of Site 783 on the west flank of a seamount on the inner wall of the Izu-Bonin trench.

The section from Samples 125-784A-13R-CC to 125-784A-22R-CC is assigned to the upper Miocene, and the interval from Samples 125-784A-22R-CC to 125-784A-31R-CC is dated as middle Miocene based on the diatoms. Unfortunately, calcareous nannofossils were rare, absent, or nondiagnostic in the Miocene sediments. The strong dissolution of the calcareous nannofossils suggests that deposition of the sedimentary interval probably took place at or below the carbonate compensation depth.

Site 786

Site 786 is located in the center of Izu-bonin forearc basin, about 120 km east of the active arc volcano of Myojin Sho, and about 70 km west of the axis of the Izu-Bonin trench.

The sediments recovered here are assigned to four lithostratigraphic units. Units I through III are defined only in Hole 786A. Unit IV, comprising massive and brecciated flows as well as ash flows, was found in both Holes 786A and 786B. The sediments are at 103.25 m below seafloor (mbsf) in Hole 786A, ranging from Pleistocene to middle Eocene in age (Fig. 2).

Four unconformities have been identified in the succession: one is located between the middle and upper Miocene, the second within the middle Miocene, the third between the upper Oligocene and middle Miocene, and the last one within the lower Oligocene.

Hole 786A

Miocene

Common to abundant, moderately preserved nannofossil assemblages were detected from Samples 125-786A-4X-1, 96–97 cm, to 125-786A-9X-5, 40 cm (Table 4).

The upper upper Miocene is recognized by the occurrence of *Discoaster berggrenii*, *Discoaster quinqueramus*, and *Triquetrorhabdulus rugosus* from Samples 125-786A-5X-CC to 125-786A-4X-1, 96–97 cm, which is equivalent to the *D. quinqueramus* Zone (CN9).

Subzone CN9a can be recognized by the FO of *Discoaster berggrenii* at the base (Sample 125-786A-5X-CC) and the FO of *Amaurolithus primus* as its top (Sample 125-786A-4X-CC). As in Hole 782A, the FO of *Ceratolithus acutus* (Sample 125-786A-3H-CC) follows directly the LO of *Discoaster quinqueramus* (Sample 125-786A-4X-1, 96–97 cm), but the subzone (CN10a) delineated by these two datums, if it exists here, falls between Cores 125-786A-3H and 125-786A-4X. At that point in the drilling process, the decision was made to switch from the hydraulic piston core (HPC) system to the XCB.

As discussed in the previous two sections, our failure to detect Subzone CN10a could be the result of one or more of the following reasons: (1) the subzone does not exist in this region; (2) *Discoaster quinqueramus* was reworked upward, thus obscuring this "gap" subzone; (3) the subzone is of too short a duration to be detected in this section; (4) the critical interval of sediment was lost when the coring system was switched from the HPC to the XCB; and (5) there is a minor hiatus at this level at this site. Based on the nannofossil evidence alone, we cannot provide a more definitive answer on this issue.

The section from Samples 125-786A-6X-2, 70 cm, through 125-786A-6X-1, 51–52 cm, is assigned to Zones CN6 to CN7 by the occurrence of *Catinaster coalitus* and *Catinaster calyculus*, but *Dis-*

coaster hamatus was not found here. Both *Catinaster coalitus* and *Catinaster calyculus* disappear simultaneously at the same level (Sample 125-786A-6X-1, 51–52 cm), at the base of Zone CN9 (Sample 125-786A-5X-CC); a hiatus, therefore, is evidently present. A similar hiatus was present in Hole 782A. A hiatus may also be present at the base of the interval of the combined Zones CN6/CN7, because *C. coalitus* and *C. calyculus* first appear together in Sample 125-786A-6X-2, 70 cm, instead of in sequence as in Hole 782A.

Subzone CN5b was detected by the rare and sporadic occurrence of *Discoaster kugleri* associated with *Discoaster variabilis*, *Cyclicargolithus floridanus* (lowermost portion of zone), and *Reticulofenestra pseudoumbilica*. Subzone CN5a, however, is missing based on the appearance of the marker species *Discoaster kugleri* right above the LO of *Sphenolithus heteromorphus* (i.e., Subzone CN5b overlain directly by Zone CN4).

The interval from Samples 125-786A-8X-1, 35–36 cm, to 125-786A-9X-5, 57–58 cm, was assigned to Zone CN4 by the presence of *Sphenolithus heteromorphus* and the absence of *Helicosphaera ampliaperita*.

A hiatus between the upper Oligocene and middle Miocene is also observed in this hole as in Hole 782A. It is evidenced by the absence of Subzone CN1b and Zones CN2 and CN3. Subzone CN1a and Zone CN4 are delimited by the LO of *Reticulofenestra bisecta* in Sample 125-786A-9X-5, 62 cm, and the FOs of *Sphenolithus heteromorphus* and *Reticulofenestra pseudoumbilica* in Sample 125-786A-9X-5, 57–58 cm, respectively (Fig. 3).

Significantly, the hiatus is marked by a strong color change in Section 125-786A-9X-5. The sediment changes from gray and greenish gray below to reddish brown about at 56–66 cm (Fig. 4).

Oligocene

Oligocene calcareous nannofossil assemblages were observed in the interval from Samples 125-786A-10X-CC to 125-786A-9X-5, 62–63 cm. The nannofossils are moderately to well preserved with slight to moderate overgrowths.

Subzone CN1a is present from the LO of *Sphenolithus ciperoensis* in Sample 125-786A-9X-5, 80 cm, to the FO of *Reticulofenestra bisecta* in Sample 125-786A-9X-5, 62–63 cm. The LO of the acme of *Cyclicargolithus f. abisectus* n. comb., which is an indicator for the top of Subzone CN1a by the Bukry zonation, extends to middle Miocene CN5 Zone (Sample 125-786A-7X-CC). It is apparent that the use of this datum for the recognition of the Subzone CN1a/CN1b boundary is not reliable, at least in these middle latitudes.

The section from Samples 125-786A-10X-3, 14–15 cm, through 125-786A-9X-6, 14–15 cm, is assigned to Zone CP19 by the occurrence of *Sphenolithus ciperoensis* together with common *Discoaster deflandrei*, *Reticulofenestra bisecta*, *Sphenolithus predistentus*, and *Triquetrorhabdulus milowii*. The boundary between Subzones CP19a and CP19b is located within the interval from Samples 125-786A-10X-3, 14–15 cm, to 125-786A-10X-2, 14–15 cm, by the LO of *Sphenolithus distentus*.

Clausicoccus fenestratus and *Reticulofenestra umbilica* occur just below Zone CP19 from Sample 125-786A-10X-4, 14–15 cm, and *Coccolithus formosus* occurs near this level (Sample 125-786A-10X-5, 14–15 cm). It is, therefore, apparent that Subzone CP16c through Zone CP18 is missing and a hiatus is present between Samples 125-786A-10X-3, 14–15 cm, and 125-786A-10X-4, 14–15 cm. The duration of the hiatus is dated at about 4.7 m.y. according to Berggren et al. (1985a).

Subzone CP16a, observed from Samples 125-786A-10X-4, 14–15 cm, to 125-786A-10X-CC, is characterized by the occurrence of *Coccolithus formosus*, *Clausicoccus fenestratus*, *Reticulofenestra umbilica*, *Isthmolithus recurvus*, and *Sphenolithus predistentus*. The FO of *Sphenolithus distentus* here extends downward to Subzone CP16, lower than Bukry's (1973) record for this occur-

rence in CP18. Therefore, *S. distentus* overlaps the upper range of *Reticulofenestra umbilica* and *Coccolithus formosus* in this hole.

The boundary between the upper Eocene and lower Oligocene (CP15/CP16) is placed between Samples 125-786A-10X-CC and 125-786A-11X-1, 8–10 cm.

Eocene

Nannofossil preservation is moderate with slight overgrowth.

Discoaster barbadiensis and *Discoaster saipanensis* are present in Sample 125-786A-11X-1, 8–10 cm, dating the sample as late Eocene. The base of Zone CP15 was detected by the FO of *Chiasmolithus oamaruensis* in Sample 125-786A-11X-2, 70 cm. Zone CP15 is divided into Subzones CP15a and CP15b by the FO of *Isthmolithus recurvus* in Sample 125-786A-11X-2, 62–64 cm, but Subzone CP15a is only 6 cm thick (Section 125-786A-11X-2, 64–70 cm).

The *Reticulofenestra umbilica* Zone (CP14) is traditionally delimited by the FO of *Reticulofenestra umbilica* at its base and the LO of *Chiasmolithus grandis* and the FO of *Chiasmolithus oamaruensis* as its top. In the absence of *C. solitus* in our volcanic-rich sediment, the CP14a/CP14b boundary is recognized within the interval from Samples 125-786A-11X-5, 65–66 cm, to 125-786A-11X-4, 120 cm, based on the FO of *Reticulofenestra bisecta*. The interval of Zone CP14 was observed from Samples 125-786A-12X-1, 40 cm, to 125-786A-11X-2, 58–59 cm.

Chiasmolithus solitus, *Coccolithus formosus*, *Cyclicargolithus f. floridanus*, and *Discoaster barbadiensis* are present and *Chiasmolithus gigas* (marker species of Subzone CP13b) is absent in the section from Samples 125-786A-12X-1, 85 cm, to 125-786A-19X-CC, which may be assigned to Subzone CP13c (dated as 44.4–47.0 Ma according to Berggren et al., 1985a). These middle Eocene sediments are underlain by volcanic basement.

Hole 786B

Drilling at Hole 786B penetrated more than 700 m into massive, brecciated, and pillowed lavas. Rare, poorly to moderately preserved calcareous nannofossils were found in sediments interbedded within the lava.

Samples 125-786B-2R-1, 50 cm, 125-786B-27R-2, 28 cm, and 125-786B-40R-1, 35 cm, are middle to late Eocene in age (Zone CP14–15), based on the presence of the marker species *Discoaster barbadiensis*, *Discoaster saipanensis*, and *Reticulofenestra umbilica* together with *Cyclicargolithus f. floridanus* and *Discoaster deflandrei*.

Nannofossil assemblages were also found from Samples 125-786B-41R-3, 60 cm, 125-786B-49R-1, 50 cm, 125-786B-51R-2, 10 cm, and 125-786B-56R-CC. The occurrence of *Coccolithus formosus*, *Reticulofenestra bisecta*, and *Cyclicargolithus f. floridanus*, which were also recovered from samples above, may confine the assemblage to the middle to upper Eocene because no other marker species were found.

Discoaster barbadiensis, *Discoaster distinctus*, and *Sphenolithus* sp. have been found from Samples 125-786B-61R-6, 26 cm, and 125-786B-63R-1, 92 cm, but the age of these Eocene samples cannot be determined.

DISCUSSION

Biochronology and Species Events

The magnetostratigraphy of Hole 782A was worked out aboard ship. Although the correlation of species events with chrons is difficult for some intervals because of the reduced recovery, correlation with the magnetic polarity time scales of Berggren et al. (1985a, 1985b) can be made. In the present study an attempt was made to tie the calcareous nannofossil datums to the Berggren et al. time scale.

Twenty-one important species from Hole 782A were selected as the calcareous nannofossil datums to correlate with magnetostratigraphy.

Table 4. Distribution of calcareous nannofossil species, Hole 786A, ODP Leg 125.

Lithologic unit	Age	Zone (Bukry, 1973, 1975)	Core, section, interval (cm)	Abundance	Preservation	<i>Amaurolithus delicatus</i>	<i>Amaurolithus primus</i>	<i>Amaurolithus tricomiculatus</i>	<i>Blackites spinosus</i>	<i>Calcidiscus leptoporus</i>	<i>Calcidiscus muccinirei</i>	<i>Calcidiscus protoammula</i>	<i>Campylophera delia</i>	<i>Catinaster calveolus</i>	<i>Catinaster coaltus</i>	
I	late Miocene	<i>Amaurolithus primus</i> Subzone (CN9b)	4X-1, 96-97	A	G	•	R	R	•	A	C	•	•	•	•	
			4X-2, 12-13	A	G	R	R	•	•	A	C	•	•	•	•	
			4X-CC, 23-24	A	G	R	R	•	•	A	C	•	•	•	•	
			4X-CC	A	G	R	R	•	•	A	C	•	•	•	•	
		<i>Discoaster berggrenii</i> Subzone (CN9a)	5X-1, 131-132	A	G	F	•	•	•	A	A	•	•	•	•	
			5X-2, 25-26	C	M	•	•	•	•	R	C	•	•	•	•	
	5X-3, 25-26		A	G	•	•	•	•	•	C	•	•	•	•		
	5X-4, 56-57		A	G	•	•	•	•	•	C	F	•	•	•		
	5X-CC		R	M	•	•	•	•	•	•	•	•	•	•		
	6X-1, 51-52		A	M	•	•	•	•	•	•	F	•	•	R	F	
	middle Miocene	<i>Catinaster coaltus</i> - <i>Discoaster humatus</i> Zones (CN6 - CN7)	6X-2, 51-52	F	M	•	•	•	•	•	•	•	•	•	R	R
			6X-2, 70	A	G	•	•	•	•	F	F	•	•	•	F	C
			6X-3, 51-52	R	M	•	•	•	•	•	•	•	•	•	•	•
			6X-4, 51-52	R	M	•	•	•	•	•	•	•	•	•	•	•
			6X-5, 33-35	F	P	•	•	•	•	•	•	•	•	•	•	•
			6X-CC	A	G	•	•	•	•	•	•	F	•	•	•	•
		<i>Discoaster kugleri</i> Subzone (CN5b)	7X-1, 88-89	C	M	•	•	•	•	•	•	R	•	•	•	•
			7X-2, 88-89	F	M	•	•	•	•	•	•	R	•	•	•	•
			7X-3, 88-89	F	P	•	•	•	•	•	•	R	•	•	•	•
			7X-4, 88-89	C	M	•	•	•	•	•	•	R	•	•	•	•
			7X-5, 88-89	C	M	•	•	•	•	•	•	R	•	•	•	•
			7X-CC	A	M	•	•	•	•	•	•	R	F	•	•	•
	<i>Helicosphaera ampliapertura</i> - <i>Sphenolithus heteromorphus</i> Zones (CP3 - CP4)	8X-1, 35-36	A	M	•	•	•	•	•	•	F	•	•	•	•	
		8X-CC	A	G	•	•	•	•	•	•	•	•	•	•	•	
9X-1, 36-37		C	M	•	•	•	•	•	•	•	•	•	•	•		
9X-2, 84-85		C	M	•	•	•	•	•	•	•	•	•	•	•		
9X-3, 40-41		F	M	•	•	•	•	•	•	•	•	•	•	•		
9X-4, 45-46		F	M	•	•	•	•	•	•	•	•	•	•	•		
9X-5, 30-31		C	M	•	•	•	•	•	•	•	•	•	•	•		
9X-5, 40		C	M	•	•	•	•	•	•	•	•	•	•	•		
9X-5, 49-50		A	M	•	•	•	•	•	•	•	•	•	•	•		
9X-5, 57-58		C	M	•	•	•	•	•	•	•	•	•	•	•		
II		late Oligocene	<i>Cyclicargolithus abisectus</i> Subzone (CN1a)	9X-5, 62-63	F	M	•	•	•	•	•	•	•	•	•	
				9X-5, 68-69	R	M	•	•	•	•	•	•	•	•	•	
	9X-5, 80			A	M	•	•	•	•	•	•	•	•	•		
	<i>Sphenolithus ciperensis</i> Zone (CP19)		9X-6, 14-15	A	M	•	•	•	•	•	•	•	•	•	•	
			9X-CC	A	G	•	•	•	•	•	•	•	•	•	•	
			10X-1, 10-11	A	G	•	•	•	•	•	•	•	•	•	•	
	early Oligocene	<i>Clausicoccus fenestratus</i> - <i>Coccolithus formosus</i> Subzones (CP16a - CP16b)	10X-2, 14-15	A	M	•	•	•	•	•	•	•	•	•		
			10X-3, 14-15	A	G	•	•	•	•	•	•	•	•	•		
			10X-4, 14-15	A	G	•	•	•	•	•	•	•	•	•		
			10X-5, 14-15	A	G	•	•	•	•	R	•	•	•	•		
			10X-6, 14-15	A	G	•	•	•	•	R	•	•	•	•		
			10X-6, 51-53	A	G	•	•	•	•	R	•	•	•	•		
	late Eocene	<i>Discoaster barbudiensis</i> Zone (CP15)	10X-CC	A	M	•	•	•	•	F	•	•	•	•		
			11X-1, 8-10	A	M	•	•	•	•	•	•	•	•	•		
			11X-1, 54-55	A	M	•	•	•	•	•	•	•	•	•		
			11X-1, 70	C	M	•	•	•	•	R	•	•	•	•		
			11X-2, 62-64	C	G	•	•	•	•	•	•	•	•	•		
			11X-2, 70	C	M	•	•	•	•	•	•	•	R	•		
III	middle Eocene	<i>Discoaster saipanensis</i> Subzone (CP14b)	11X-3, 58-59	A	M	•	•	•	R	•	•	•	•			
			11X-3, 70	C	M	•	•	•	R	•	•	•	•			
			11X-4, 62-63	A	M	•	•	•	R	•	•	•	•			
			11X-4, 90	A	M	•	•	•	R	•	•	•	•			
			11X-4, 120	A	M	•	•	•	R	•	•	R	•			
			11X-5, 65-66	A	M	•	•	•	R	•	•	•	•			
	<i>Discoaster bifax</i> Subzone (CP14a)	11X-5, 131-132	C	M	•	•	•	•	•	•	•	R	•			
		11X-5, 135	A	G	•	•	•	•	•	•	•	•	R			
		11X-6, 57-58	R	M	•	•	•	•	•	•	•	•	•			
		11X-6, 30	A	G	•	•	•	•	F	•	R	•	•			
		11X-CC	A	M	•	•	•	•	•	•	•	•	R			
		12X-1, 40	C	M	•	•	•	•	•	•	•	•	R			
IV	<i>Coccolithus staurion</i> Subzone (CP13c)	12X-1, 85	C	M	•	•	•	•	•	•	•	•	R			
		12X-1, 135	F	M	•	•	•	•	•	•	•	•	•			
		12X-1, 145	R	M	•	•	•	•	•	•	•	•	•			
		12X-2, 15	C	M	•	•	•	•	•	•	•	•	R			
		12X-2, 32-33	A	M	•	•	•	•	•	•	•	•	R			
		12X-2, 35	A	M	•	•	•	•	•	•	•	R	•			
15X-CC	R	P	•	•	•	•	•	•	•	•	•					
16X-CC	R	P	•	•	•	•	•	•	•	•	•					
17X-CC	R	•	•	•	•	•	•	•	•	•	•					
19X-CC	R	M	•	•	•	•	•	•	•	•	R					

Note: Abundance: A = abundant, C = common, F = few, R = rare. Preservation: G = good, M = moderate, P = poor.

Table 4 (continued).

<i>Reticulofenestra hillae</i>	<i>Reticulofenestra minutula</i>	<i>Reticulofenestra pseudumbillica</i>	<i>Reticulofenestra reticulata</i>	<i>Reticulofenestra samoderovii</i>	<i>Reticulofenestra umbillica</i>	<i>Sphenolithus ciperensis</i>	<i>Sphenolithus distentus</i>	<i>Sphenolithus furcatolithoides</i>	<i>Sphenolithus heteromorphus</i>	<i>Sphenolithus intercalaris</i>	<i>Sphenolithus moriformis</i>	<i>Sphenolithus predictentus</i>	<i>Sphenolithus pseudoradians</i>	<i>Sphenolithus radians</i>	<i>Sphenolithus springer</i>	<i>Thoracosphaera</i> spp.	<i>Triquetrorhabdulus carinatus</i>	<i>Triquetrorhabdulus millowii</i>	<i>Triquetrorhabdulus rugosus</i>	<i>Umbilicosphaera sibogae</i>	<i>Zygabolithus bijugatus</i>	
.	.	A	R	R	.	4X-1, 96-97	
.	.	A	R	4X-2, 12-13	
.	.	A	R	4X-CC, 23-24	
.	.	A	R	4X-CC	
.	.	A	C	R	.	5X-1, 131-132	
.	.	C	F	R	F	5X-2, 25-26	
.	R	A	A	F	R	.	5X-3, 25-26	
.	R	A	A	5X-4, 56-57	
.	F	A	A	5X-CC	
.	F	A	A	R	R	.	6X-1, 51-52	
.	R	A	A	R	.	.	6X-2, 51-52	
.	R	A	A	R	.	.	6X-2, 70	
.	F	A	A	6X-3, 51-52	
.	F	A	A	6X-4, 51-52	
.	R	A	A	6X-5, 33-35	
.	R	A	A	6X-CC	
.	R	A	A	7X-1, 88-89	
.	R	A	A	7X-2, 88-89	
.	R	A	A	7X-3, 88-89	
.	R	A	A	R	.	.	.	7X-4, 88-89	
.	R	A	A	R	.	.	.	7X-5, 88-89	
.	R	A	A	7X-CC	
.	F	A	A	R	.	R	.	R	8X-1, 35-36	
.	F	A	A	R	.	R	.	R	8X-CC	
.	F	A	A	R	.	R	.	R	9X-1, 36-37	
.	F	A	A	R	.	R	.	R	9X-2, 84-85	
.	F	A	A	R	.	R	.	R	9X-3, 40-41	
.	F	A	A	R	.	R	.	R	9X-4, 45-46	
.	F	A	A	R	.	R	.	R	9X-5, 30-31	
.	F	A	A	R	.	R	.	R	9X-5, 40	
.	F	A	A	R	.	R	.	R	9X-5, 49-50	
.	F	A	A	R	.	R	.	R	.	.	.	R	R	.	.	9X-5, 57-58	
.	F	A	A	R	.	R	.	R	.	.	.	R	R	.	.	9X-5, 62-63	
.	F	A	A	R	.	R	.	R	.	.	.	R	R	.	.	9X-5, 68-69	
.	F	A	A	R	.	R	.	R	.	.	.	R	R	.	.	9X-5, 80	
.	F	A	A	.	.	R	F	.	R	.	F	.	R	.	.	.	R	R	.	.	9X-6, 14-15	
.	F	A	A	.	.	R	F	.	R	.	F	.	R	.	.	.	R	R	.	.	9X-CC	
.	F	A	A	.	.	R	F	.	R	.	F	.	R	.	.	.	R	R	.	.	10X-1, 10-11	
.	F	A	A	.	.	R	F	.	R	.	F	.	R	.	.	.	R	R	.	.	10X-2, 14-15	
.	F	A	A	.	.	R	F	.	R	.	F	.	R	.	.	.	R	R	.	.	10X-3, 14-15	
.	F	A	A	.	.	R	F	.	R	.	F	.	R	.	.	.	R	R	.	.	10X-4, 14-15	
.	F	A	A	.	.	R	F	.	R	.	F	.	R	.	.	.	R	R	.	.	10X-5, 14-15	
.	F	A	A	.	.	R	F	.	R	.	F	.	R	.	.	.	R	R	.	R	10X-6, 14-15	
.	F	A	A	.	.	R	F	.	R	.	F	.	R	.	.	.	R	R	.	R	10X-6, 51-53	
.	F	A	A	.	.	R	F	.	R	.	F	.	R	.	.	.	R	R	.	R	10X-CC	
.	F	A	A	.	.	R	F	.	R	.	F	.	R	.	.	.	R	R	.	R	11X-1, 8-10	
.	F	A	A	.	.	R	F	.	R	.	F	.	R	.	.	.	R	R	.	R	11X-1, 54-55	
.	F	A	A	.	.	R	F	.	R	.	F	.	R	.	.	.	R	R	.	R	11X-1, 70	
.	F	A	A	.	.	R	F	.	R	.	F	.	R	.	.	.	R	R	.	R	11X-2, 62-64	
.	F	A	A	.	.	R	F	.	R	.	F	.	R	.	.	.	R	R	.	R	11X-2, 70	
.	F	A	A	.	.	R	F	.	R	.	F	.	R	.	.	.	R	R	.	R	11X-3, 58-59	
.	F	A	A	.	.	R	F	.	R	.	F	.	R	.	.	.	R	R	.	R	11X-3, 70	
.	F	A	A	.	.	R	F	.	R	.	F	.	R	.	.	.	R	R	.	R	11X-4, 62-63	
.	F	A	A	.	.	R	F	.	R	.	F	.	R	.	.	.	R	R	.	R	11X-4, 90	
.	F	A	A	.	.	R	F	.	R	.	F	.	R	.	.	F	.	R	R	.	11X-4, 120	
.	F	A	A	.	.	R	F	.	R	.	F	.	R	.	.	.	R	R	.	F	11X-5, 65-66	
.	F	A	A	.	.	R	F	.	R	.	F	.	R	.	F	.	R	R	.	.	11X-5, 131-132	
.	F	A	A	.	.	R	F	.	R	.	F	.	R	.	R	.	R	R	.	.	11X-5, 135	
.	F	A	A	.	.	R	F	.	R	.	F	.	R	.	R	.	R	R	.	.	11X-6, 57-58	
.	F	A	A	.	.	R	F	.	R	.	F	.	R	.	R	.	R	R	.	.	11X-6, 30	
.	F	A	A	.	.	R	F	.	R	.	F	.	R	.	R	.	R	R	.	.	11X-CC	
.	F	A	A	.	.	R	F	.	R	.	F	.	R	.	R	.	R	R	.	.	12X-1, 40	
.	F	A	A	.	.	R	F	.	R	.	F	.	R	.	R	.	R	R	.	.	12X-1, 85	
.	F	A	A	.	.	R	F	.	R	.	F	.	R	.	R	.	R	R	.	.	12X-1, 135	
.	F	A	A	.	.	R	F	.	R	.	F	.	R	.	R	.	R	R	.	.	12X-1, 145	
.	F	A	A	.	.	R	F	.	R	.	F	.	R	.	R	.	R	R	.	.	12X-2, 15	
.	F	A	A	.	.	R	F	.	R	.	F	.	R	.	R	.	R	R	.	.	12X-2, 32-33	
.	F	A	A	.	.	R	F	.	R	.	F	.	R	.	R	.	R	R	.	.	12X-2, 35	
.	F	A	A	.	.	R	F	.	R	.	F	.	R	.	R	.	R	R	.	.	12X-CC	
.	F	A	A	.	.	R	F	.	R	.	F	.	R	.	R	.	R	R	.	.	15X-CC	
.	F	A	A	.	.	R	F	.	R	.	F	.	R	.	R	.	R	R	.	.	16X-CC	
.	F	A	A	.	.	R	F	.	R	.	F	.	R	.	R	.	R	R	.	.	17X-CC	
.	F	A	A	.	.	R	F	.	R	.	F	.	R	.	R	.	R	R	.	.	19X-CC	

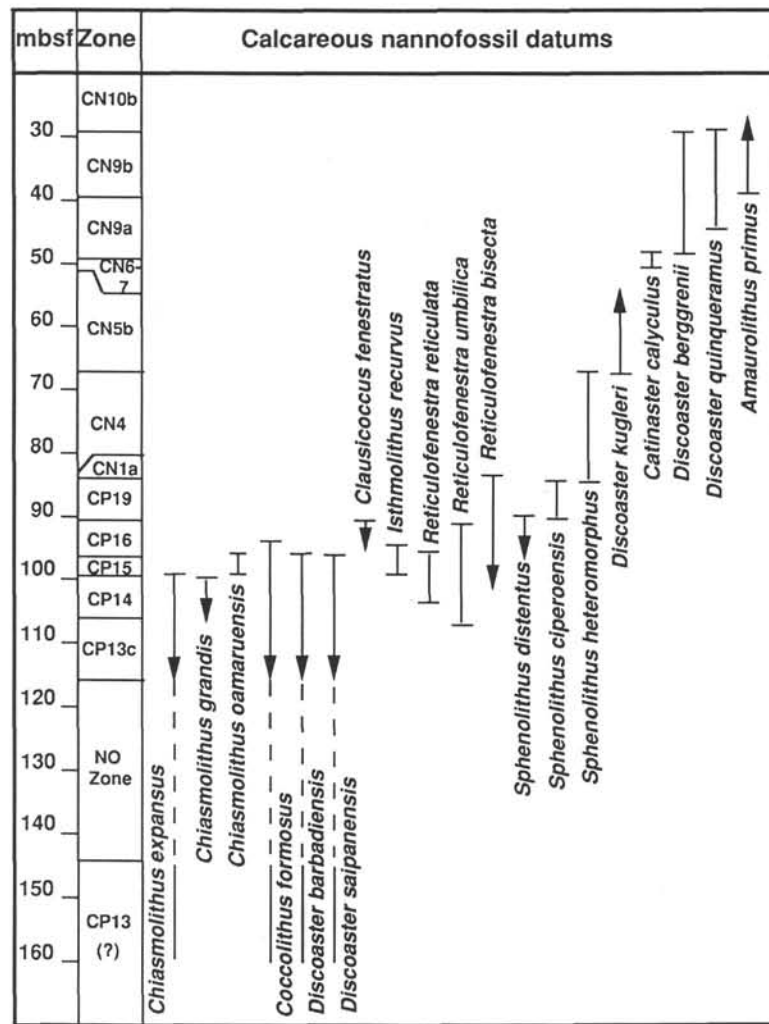


Figure 3. Summary of biostratigraphy and species datums for Hole 786A.

ogy (Table 5). The results indicate that the datum levels for most species in general correspond well with the magnetic polarity stratigraphies of Berggren et al. (1985a, 1985b). In some cases, however, datum levels fall within different zones than those generally reported in the literature. These are discussed in the following.

Reticulofenestra reticulata

Reticulofenestra reticulata has been reported from middle to upper Eocene sediments of different marine environments and latitudes (Gallagher, 1989; Pujos-Lamy, 1987), but the biostratigraphic range of this species varies from one region to the next. Wei and Wise (1989) reported that the LO of *Reticulofenestra reticulata* was located at the bottom of Subchron C15N, dated as 37.6 Ma, and that the FO of this species occurred at the bottom of Chron C18 (43.6 Ma) from Site 516, in the South Atlantic Ocean. This species, however, was found in the study area ranging from Chrons C15 to C17 (Zone CP14-15) in Hole 782A. It is likely that the FO of *Reticulofenestra reticulata* is not coeval in different areas, but the LO of this species is probably synchronous (Fig. 5).

Reticulofenestra reticulata is round in shape and has a distinct central area structure. Wei and Wise (1990) have suggested that the size of this taxon increases upsection. The results of a detailed morphometric study of Leg 125 material reveal that in general this is

true. The earlier forms are smaller, and the later ones are larger. Figure 6 shows that the size ranges from 4 to 11 μm in diameter, and that most of the early specimens (Zone CP14) are 6–8 μm whereas most later specimens (Zone CP15) are 8–11 μm . Further statistical study of the size of *Reticulofenestra reticulata* may help to separate Zone CP14 from Zone CP15.

Sphenolithus distentus

The FO of *Sphenolithus distentus*, used as a marker species for the Zone CP17/CP18 boundary by Okada and Bukry (1980), is located at the bottom of C12N in Hole 782A. This datum coincides with the information given by Berggren et al. (1985a) (about 34.2 Ma). In Hole 782A, however, the FO of *Sphenolithus distentus* overlaps the upper ranges of *Reticulofenestra umbilica* and *Coccolithus formosus*, which extends this datum downward into Subzone CP16b. The overlap with these three species mentioned previously was also reported from the Southern Hemisphere (Wei and Wise, 1989; see discussion and references therein). It is apparent that the FO of *Sphenolithus distentus* is not a reliable datum (Fig. 5).

The LO of *Sphenolithus distentus*, used as the Subzone CP19a/CP19b boundary by both Martini (1971) and Okada and Bukry (1980), is a reliable marker based on the present study of Holes 782A and 786A (about 28.5 Ma).

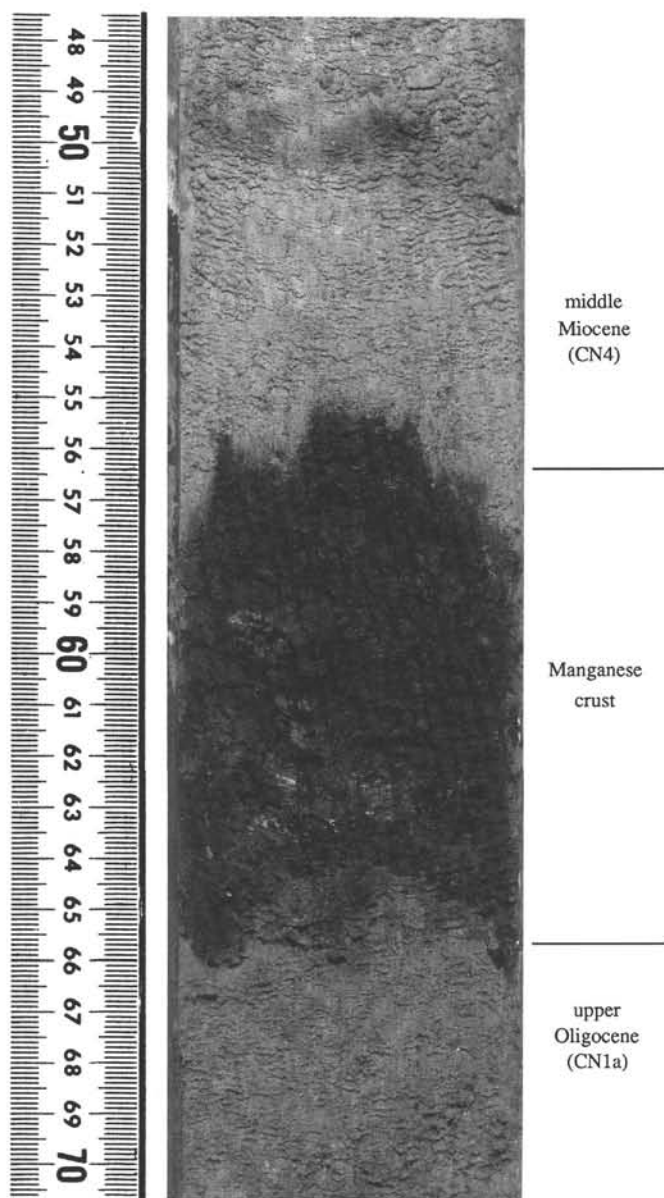


Figure 4. Lithologic change at the contact between the upper Oligocene and middle Miocene, Section 125-786A-9X-5, 50–70 cm.

Reticulofenestra bisecta

A marker species for the CP19b/CN1a boundary according to Bukry's (1973, 1975) zonation, the LO of this taxon was located at anomaly 6C of the geomagnetic polarity time scale (23.7 Ma) according to Berggren (1985a).

The LO of *Reticulofenestra bisecta* was observed on the top of anomaly 6C of the geomagnetic polarity time scale (23.5 Ma) in the present study, higher than that of Berggren et al. (1985a) and higher than the LO of *Sphenolithus ciproensis* (Fig. 5). As a result, the LO of the species may be used to recognize the Subzone CN1a/CN1b boundary in lieu of the end of the acme of *Cyclicargolithus f. abisectus* n. comb. (see following discussion). The same situation was observed at Hole 786A. Therefore, we believe that the LO of *Reticulofenestra bisecta* is probably a reasonable nannofossil marker to approximate the Oligocene/Miocene boundary based on the present study and other updated information (Biolzi, 1985; Berggren et al., 1985a).

Table 5. Summary of biochronological properties of selected nannofossil species events determined for Hole 782A compared with values given by Berggren et al. (1985a, 1985b).

Species events		Depth (mbsf)	Age (Ma)	Ma (Berggren et al., 1985 a, b)
LO	<i>Chiasmolithus grandis</i>			
	<i>Chiasmolithus expansus</i>	385.13	40.0	40.0
LO	<i>Coccolithus formosus</i>	370.50	35.0	35.1
LO	<i>Reticulofenestra reticulata</i>	375.16	37.0	
LO	<i>Discoaster barbadiensis</i>	375.16	37.0	36.7
LO	<i>Discoaster saipanensis</i>	375.16	37.0	36.7
FO	<i>Reticulofenestra umbilica</i>	390.52	>40.0	46.0
LO	<i>Reticulofenestra bisecta</i>	330.04	23.5	23.7
FO	<i>Sphenolithus ciproensis</i>	361.18		30.2
LO	<i>Sphenolithus ciproensis</i>	331.85	25.0	25.2
FO	<i>Chiasmolithus oamaruensis</i>	383.80	39.8	39.8
LO	<i>Chiasmolithus solitus</i>	389.80	>40.0	42.3
FO	<i>Isthmolithus recurvus</i>	382.81	39.6	37.8
LO	<i>Isthmolithus recurvus</i>	362.25	33.0	
LO	<i>Cyclicargolithus f. abisectus</i>	278.80	12.5	23.7
FO	<i>Sphenolithus distentus</i>	363.48	34.7	34.2
LO	<i>Sphenolithus distentus</i>	342.21	28.5	28.2
LO	<i>Sphenolithus predistentus</i>	342.21	28.5	28.2
FO	<i>Sphenolithus heteromorphus</i>	329.70		17.1
LO	<i>Sphenolithus heteromorphus</i>	312.61	14.2	14.4
FO	<i>Catinaster calyculus</i>	248.72	9.8	10.0
LO	<i>Catinaster calyculus</i>	245.72	9.0	
FO	<i>Catinaster coalitus</i>	251.09	10.2	10.3
LO	<i>Catinaster coalitus</i>	245.72	9.0	9.0
FO	<i>Discoaster kugleri</i>	278.80	12.5	13.1
LO	<i>Discoaster kugleri</i>	253.49	10.5	
FO	<i>Amaurolithus primus</i>	182.85	6.5	6.5
FO	<i>Discoaster berggrenii</i>	231.37	7.6	8.2
LO	<i>Discoaster berggrenii</i>	154.52	5.5	5.6
FO	<i>Discoaster quinqueramus</i>	242.72	8.5	8.2
LO	<i>Discoaster quinqueramus</i>	154.52	5.5	

Cyclicargolithus floridanus abisectus n. comb.

The end of the acme in the occurrence of *Cyclicargolithus f. abisectus* n. comb. marks the Subzone CP19a/CP19b boundary according to Bukry's (1973, 1975) zonation, and the LO of this acme has also been recorded at anomaly C6C (about 23.7 Ma) by Berggren et al. (1985a) and at Chron C6CN from the Mediterranean by Lowrie et al. (1982). This places the LO of this acme at the Oligocene/Miocene boundary.

Cyclicargolithus f. floridanus is very similar to *Cyclicargolithus f. abisectus* n. comb. in terms of structure under either the light microscope or SEM, and the main difference between the two species is probably due to size. *Cyclicargolithus f. floridanus* n. comb., less than 9 µm across, appears during the middle Eocene (Zone CP14) and ranges up to the middle Miocene Subzone CN5a (11.6 Ma based on Berggren et al., 1985b).

During the present study, the two species were found together in Holes 782A and 786A. *Cyclicargolithus f. floridanus* occurs from Subzone CP14b and extends through Subzone CN5a. *Cyclicargolithus f. abisectus* n. comb. also has a long range distribution. Appearing in Zone CP15, *Cyclicargolithus f. abisectus* n. comb. attains its acme in Zone CP19, but then continues to be common until Subzone CN5a. Common as well in some samples of CN5a, it finally disappears with *C. floridanus* near the top of this subzone. The LO of *Cyclicargolithus f. abisectus* n. comb. apparently varies from one area to the next based on the present study in comparison with those of Bukry (1973) and others (Lowrie et al., 1982). In addition, there was no latest Oligocene termination of the acme to mark the Oligocene/Miocene boundary at the Leg 125 sites. The stratigraphic data presented here strongly suggest that *Cyclicargolithus f. abisectus* n. comb. is a large-sized variant of *Cyclicargolithus floridanus* (Fig. 5). It is, therefore, reduced to subspecies rank (see following section). It could possibly be an ecologic

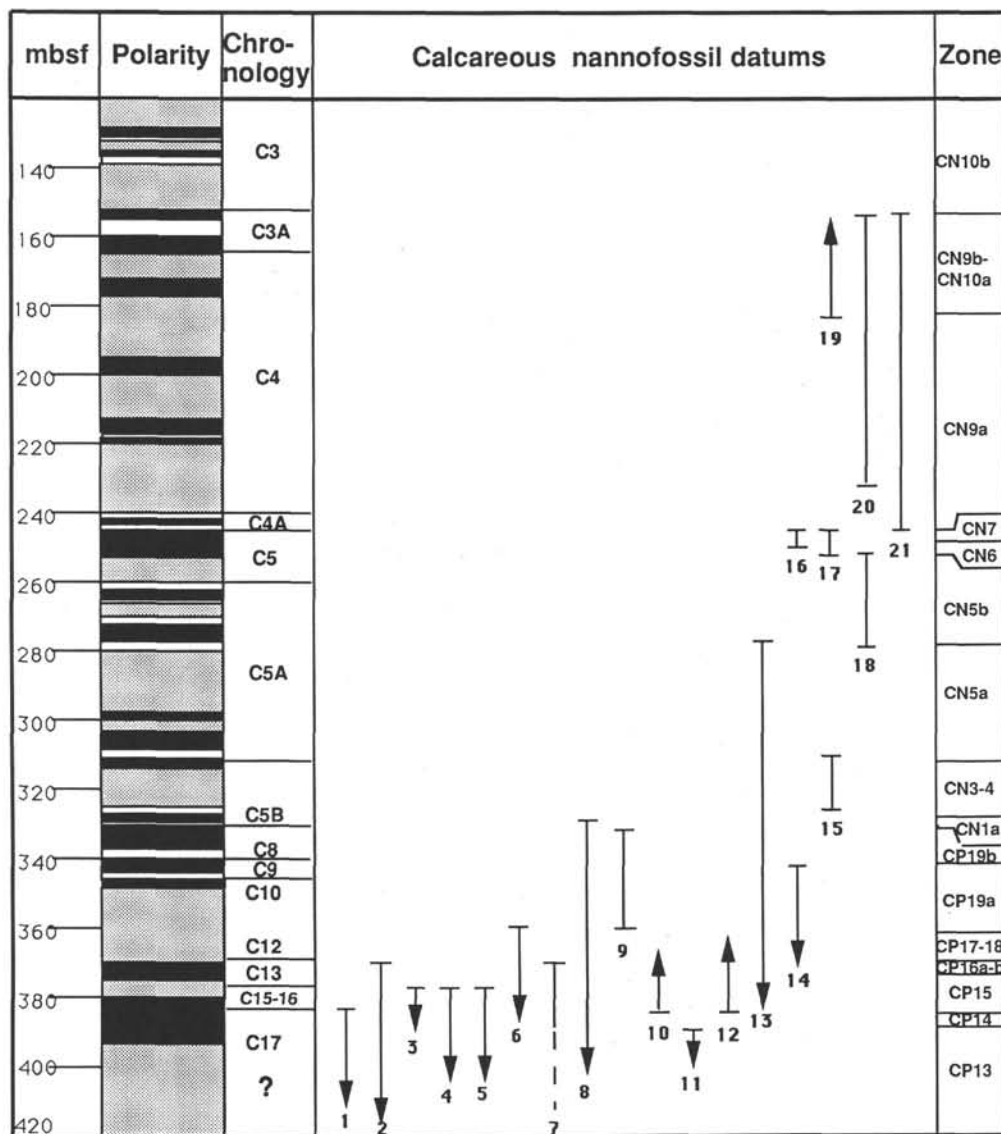


Figure 5. Magnetobiostratigraphy of Hole 782A: comparison of the results from this study and those of Berggren et al. (1985a, 1985b). The stippled parts in the polarity column indicate indeterminate or no recovery. 1. *Chiasmolithus grandis* and *Chiasmolithus expansus*, 2. *Coccolithus formosus*, 3. *Reticulofenestra reticulata*, 4. *Discoaster barbadiensis*, 5. *Discoaster saipanensis*, 6. *Helicosphaera compacta*, 7. *Reticulofenestra umbilica*, 8. *Reticulofenestra bisecta*, 9. *Sphenolithus ciperoensis*, 10. *Chiasmolithus oamaruensis*, 11. *Chiasmolithus solitus*, 12. *Isthmolithus recurvus*, 13. *Cyclicargolithus f. abisectus*, 14. *Sphenolithus distentus*, 15. *Sphenolithus heteromorphus*, 16. *Catinaster calyculus*, 17. *Catinaster coalitus*, 18. *Discoaster kugleri*, 19. *Amaurolithus primus*, 20. *Discoaster berggrenii*, 21. *Discoaster quinqueramus*.

variant of *C. floridanus*. In any case, its stratigraphic value is quite limited except in the broadest sense, and it should not be used for refined stratigraphy.

Sediment-accumulation Rates

A curve representing the sediment-accumulation rates for Hole 782A has been constructed by dividing the thickness of the interval by the time represented (Fig. 7). The time for the interval was measured by correlation with the geomagnetic polarity time scale of Berggren et al. (1985a, 1985b), and numerical ages were assigned for each depth. The diagram shows that the sediment-accumulation rates have changed from the middle Eocene to Miocene. Four stages distinguished by different rates may be recognized from Hole 782A.

Sedimentation stage one, middle Eocene to early Oligocene in age, had an accumulation rate of about 2.3 m/m.y. The estimated rate of stage two, from late early Oligocene to late Oligocene, was about 4.5 m/m.y. as calculated from the base of two magnetostratigraphy events (B C9N and B C8R, Fig. 7). These two sediment-accumulation rates are nearly equal. One hiatus exists within the early Oligocene.

The third stage, middle Miocene in age, is estimated to be about 5.9 m/m.y., much longer than the first or second stage. The sedimentation rate for stage four increased dramatically to 33.2 m/m.y. (T C4AN and T C3AN, fig. 7) during the late Miocene.

According to these analyses the sedimentation rate increased gradually from the middle Eocene to Miocene, then dramatically from the late middle Miocene to late Miocene. The lithology in the Miocene is vitric nannofossil chalk and in the Pliocene it is nannofossil marl.

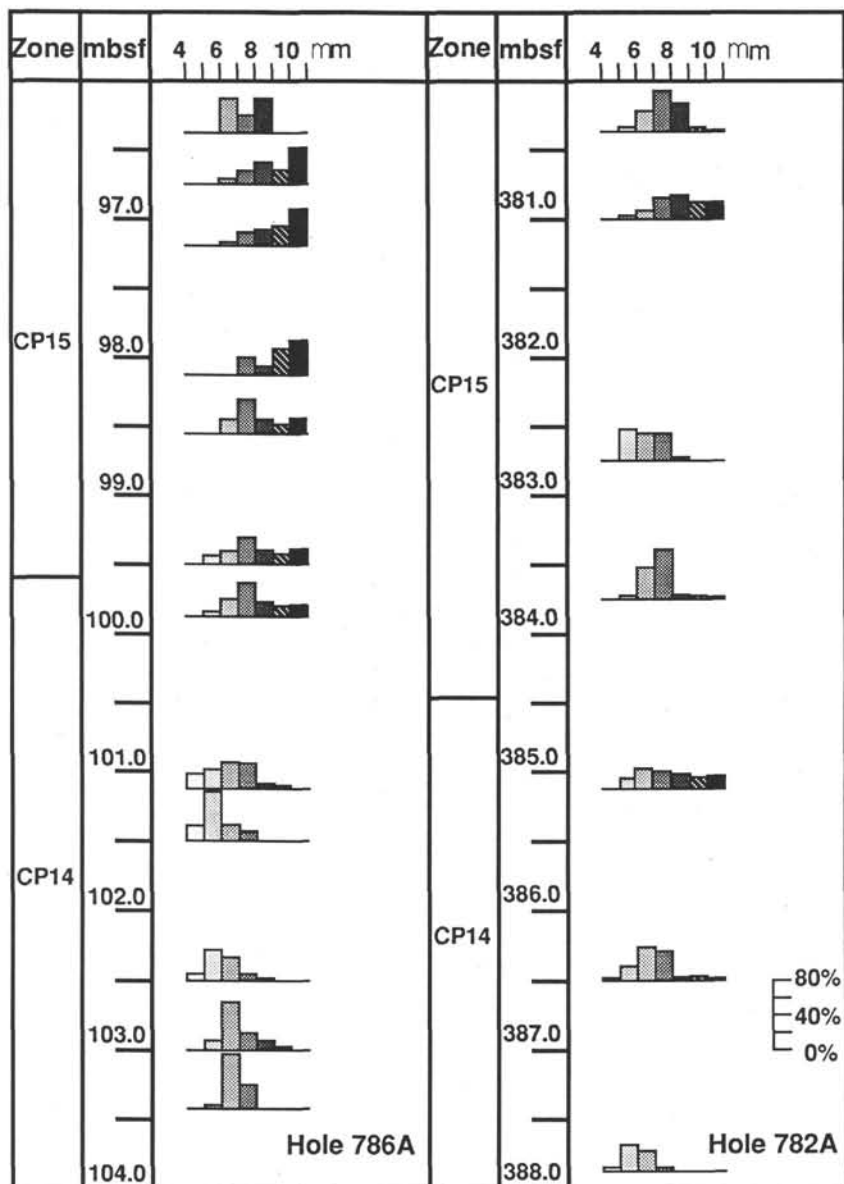


Figure 6. The size variation of *Reticulofenestra reticulata* from Zones CP14–15 based on the relative percentage of different sizes in each sample.

In conjunction with subsidence and pelagic sedimentation, this site received considerable fine volcanogenic sediment that increased the sedimentation rates. However, in Hole 786A, which is 120 km east of Hole 782A, the total coeval sediments are only 120 m thick and the Miocene is a purer nannofossil marl without the vitric component, which considerably augments the section at Site 782.

SYSTEMATIC PALEONTOLOGY

Most of the calcareous nannoplankton found on Leg 125 are well documented elsewhere and need no discussion. However, a few taxa are discussed to provide better understanding of their occurrences.

Genus *CATINASTER* Martini and Bramlette (1963)

Remarks. The genus and two species, *C. coalitus* and *C. calyculus*, were described by Martini and Bramlette (1963); the two species have

short ranges that partially overlap. In 1981, Martini also described both species from Leg 59, in the Philippine Sea. Bukry (1971) described another species of the genus, *Catinaster mexicanus*, from the Gulf of Mexico. The species was later illustrated via scanning electron microscopy by Ellis et al. (1972) from Gulf of Mexico and was reported by Müller (1974) from Leg 25, in the western Indian Ocean.

Martini (1980) suggested that the genus seems to be restricted to the middle upper Miocene and that the first species to occur is *C. coalitus*, which defines the base of his Zone NN8 (= Bukry's Zone CN6). Both *C. coalitus* and *C. calyculus* are present together in part of Zone NN8 as well as in most of the following Zone NN9 (*Discoaster hamatus* Zone). The LO of *C. coalitus* occurs prior to that of *Discoaster hamatus*, whereas *C. calyculus* extends into Zone NN10 (Bukry's Zone CN8). The situation is similar in the Leg 125 study area.

Based on Bukry's (1975) zonation, the FO of *Catinaster coalitus* is defined as the base of *Catinaster coalitus* Zone (CN6), and the FO of *Discoaster hamatus* is recognized as the base of the *Catinaster calyculus*

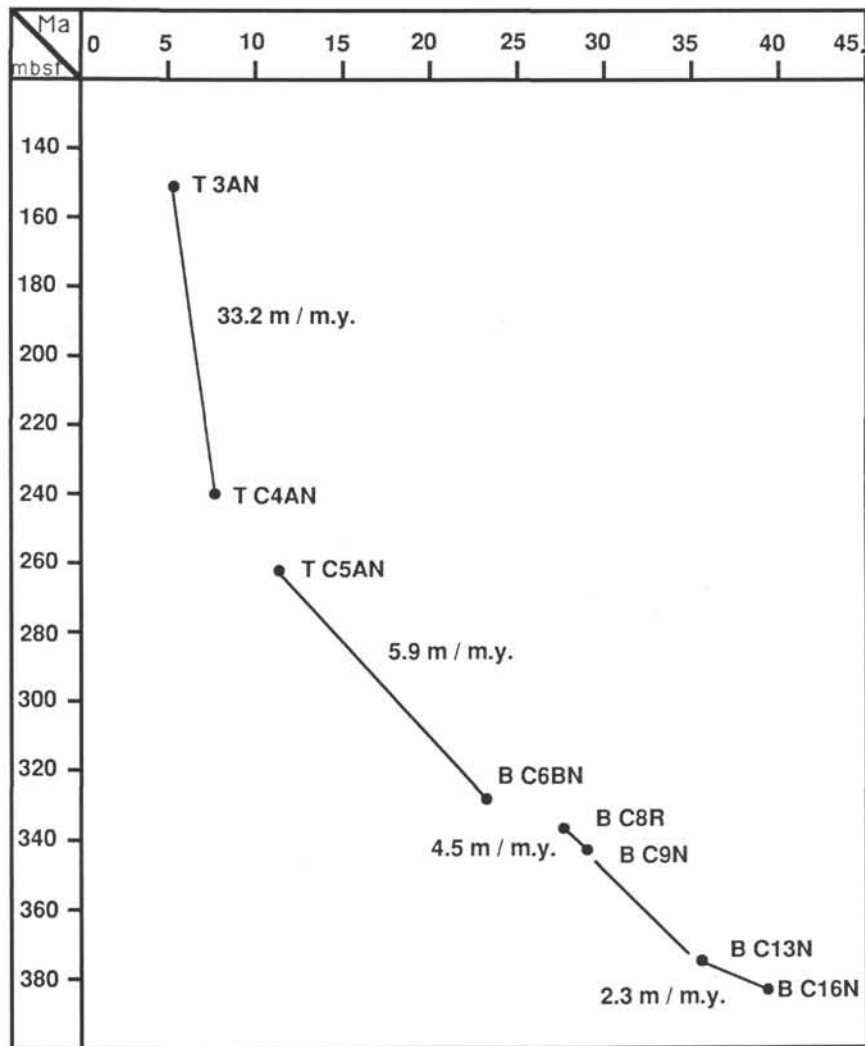


Figure 7. Sediment-accumulation rate curve for Hole 782A. Datums are the bottom (B) or top (T) of the paleomagnetic chrons.

Subzone (CN7a). In the present study, however, *Catinaster calyculus* occurs in Subzone CN6 prior to the appearance of *Discoaster hamatus*.

Assuming that the sections in question are complete, the FO of *Catinaster calyculus* relative to that of *D. hamatus*, therefore, is apparently different for different areas; it seems to occur earlier in the middle latitude western Pacific Ocean (Legs 59 and 125) than in the tropical areas described by Bukry (1975). Further research is needed to better establish these patterns of occurrence.

Catinaster coalitus Martini and Bramlette
(Pl. 5, Figs. 9–10, 17)

Remarks. *Catinaster coalitus* is six-rayed, basketlike in appearance, and round to hexagon or concave-hexagon in shape. In plan view the short rays reach the inner edge of the outer rim, and there is a depressed round area in the center. The point of junction occurs in the center of an inter-ray area and some form a small node. Late middle Miocene to early late Miocene in age.

Catinaster mexicanus Bukry
(Pl. 5, Figs. 7–8, 18)

Remarks. Small, rosette-shaped *Catinaster mexicanus* has six short bifurcate rays that reach the inner portion of the outer rim. The

large, deep, depressed central area and outer rim are formed from adjoining bifurcating rays. Early late Miocene in age.

Genus *CYCLICARGOLITHUS* Bukry (1971)

Cyclicargolithus floridanus (Roth and Hay) *abisectus* (Müller) n. comb.
(Pl. 3, Figs. 7–8; Pl. 4, Fig. 14)

Coccolithus aff. *C. bisectus* (Hay, Mohler, and Wade), Bramlette and Wilcoxon, p. 102, pl. 4, figs. 9–10.

Coccolithus? *abisectus* Müller, 1970, p. 92, pl. 9, figs. 9, 10; pl. 12, fig. 1.
Dictyococcites abisectus (Müller) Bukry and Percival, 1971, p. 127, pl. 2, figs. 9–11.

Cyclicargolithus abisectus (Müller) Wise, 1973, p. 594.

Remarks. As discussed previously, *Cyclicargolithus floridanus* and *Cyclicargolithus floridanus abisectus* n. comb. go extinct at the same level in our sections. *Cyclicargolithus f. abisectus* n. comb. is rare to common toward the top of its range in samples of nannofossil Subzone CP5a (middle middle Miocene). It is even abundant at the top of this zone in Sample 125-782A-30X-1, 54–55 cm. The persistence of these two forms to the same extinction level indicates to us that these are nothing more than variants of the same species. This conclusion is in agreement with the studies of Firth

(1989), who performed biometric analysis on this group. He concluded that *C. f. abisectus* n. comb. is simply a large size variant of *C. floridanus* that developed sometime after this plexus became established during the Eocene. *Cyclicargolithus f. abisectus* n. comb. is generally reported from assemblages of middle Oligocene age or younger, but we noted rare to common specimens up to 10 μm long in the upper Eocene of both Sites 782 and 786. Firth (1989) considered both forms to be one species, and noted that gradual increases in size are common in many fossil groups. This is clearly the case for many coccolith groups (for example, Bown, 1987; Bralower et al., 1989).

Olafsson (1989) also performed a detailed biometric analysis on this group and came to conclusions similar to those of Firth (1989). He pointed out that according to the original descriptions of the two taxa, their sizes overlap considerably and that it is virtually impossible to distinguish between them.

In the present study we distinguish specimens of *C. f. abisectus* n. comb. as an end member of the assemblage based on its size and interference pattern under crossed nicols. Included in *C. f. abisectus* n. comb. were specimens ranging in size from 9 to 12 μm . Forms up to 10 μm are rare to few in the upper Eocene at Sites 782 and 786 (Tables 3 and 4).

We did not detect an end of an acme of *C. f. abisectus* n. comb. at the top of Subzone CN1a as suggested by Bukry (1973, 1975). Instead, this form was abundant above as well as below this level, and thus this event could not be used to delimit this subzone in our sections. In addition, the extinction of both subspecies of *C. floridanus* occurred at the same level at this mid-latitude site. If the general size increase of the group is not due to genetic factors, then there may be some paleoenvironmental signal to be derived from the persistence of the *C. f. abisectus* n. comb. population in our study area. There seems to be little reliable biostratigraphic information to be gained, however, if one plots the subspecies separately, and this may not be done in our future biostratigraphic studies.

Cyclicargolithus floridanus floridanus (Roth and Hay) Bukry, 1971 (Pl. 3, Figs. 9–10; Pl. 4, Fig. 15)

Coccolithus floridanus Roth and Hay, 1967, p. 445, pl. 6, figs. 1–4.

Cyclicargolithus floridanus (Roth and Hay) Bukry, 1971, p. 312.

Reticulofenestra floridana (Roth and Hay) Theodoridis, 1984, p. 85.

ACKNOWLEDGMENTS

The study was supported by the Ocean Drilling Program and the U.S. Scientific Advisory Committee (USSAC) grant for the senior author. Lab facilities were provided by an equipment grant from the Amoco Foundation and by National Science Foundation grant DPP 89-17976 to S. W. Wise. We thank Shaozhi Mao and Melanie Carpenter for slide preparation; Kim Riddle assisted in the SEM photography.

We benefited considerably from valuable discussions with Drs. John V. Firth and Wuchang Wei and from critical reviews by Drs. P. J. Coleman and J. V. Firth. The first author would like to extend special thanks to Dr. Wise for his kind help and encouragement for my participation in Leg 125 of the Ocean Drilling Program.

REFERENCES

- Backman, J., Schneider, D. A., Rio, D., and Okada, H., 1990. Neogene low-latitude magnetostratigraphy from Site 710 and revised age estimates of Miocene nannofossil datum events. In Duncan, R. A., Backman, J., Peterson, L. C., et al., *Proc. ODP, Sci. Results*, 115: College Station, TX (Ocean Drilling Program), 271–272.
- Berggren, W. A., Kent, D. V., and Flynn, J. J., 1985a. Jurassic to Paleogene: Part 2. Paleogene geochronology and chronostratigraphy. In Snelling, N. J. (Ed.), *The Chronology of the Geological Record*. Geol. Soc. London Mem., 10:141–195.
- Berggren, W. A., Kent, D. V., and Van Couvering, J. A., 1985b. The Neogene: Part 2. Neogene geochronology and chronostratigraphy. In Snelling, N. J. (Ed.), *The Chronology of the Geological Record*. Geol. Soc. London Mem., 10:212–247.
- Biolzi, M., 1985. The Oligocene/Miocene boundary in selected Atlantic, Mediterranean and Paratethyan sections based on stratigraphic and stable isotope evidence. *Mem. Sci. Geol.*, 37:303–376.
- Bown, P. R., 1987. Taxonomy, evolution, and biostratigraphy of Late Triassic–Early Jurassic calcareous nannofossils. *Palaeontol. Assoc. London, Spec. Pap. Palaeontol.*, 38:1–118.
- Bralower, T. J., Monechi, S., and Thierstein, H. R., 1989. Calcareous nannofossil zonation of the Jurassic-Cretaceous boundary interval and correlation with the geomagnetic polarity timescale. *Mar. Micropaleontol.*, 14:153–235.
- Bukry, D., 1971. *Discoaster* evolutionary trends. *Micropaleontology*, 17:43–52.
- , 1973. Low-latitude coccolith biostratigraphic zonation. In Edgar, N. T., Saunders, J. B. et al., *Init. Repts. DSDP*, 15: Washington (U.S. Govt. Printing Office), 685–703.
- , 1975. Coccolith and silicoflagellate stratigraphy, northwestern Pacific Ocean, Deep Sea Drilling Project, Leg 32. In Larson, R. L., Moberly, R., et al., *Init. Repts. DSDP*, 32: Washington (U.S. Govt. Printing Office), 677–702.
- Ellis, C. H., 1982. Calcareous nannoplankton biostratigraphy—Deep Sea Drilling Project Leg 60. In Hussong, D. M., Uyeda, S. et al., *Init. Repts. DSDP*, 60: Washington (U.S. Govt. Printing Office), 507–535.
- Ellis, C. H., Lohmann, W. H., and Wray, J. L., 1972. Upper Cenozoic calcareous nannofossils from the Gulf of Mexico (Deep Sea Drilling Project, Leg 1, Site 3). *Colo. Sch. Mines Q.*, 67:1–103.
- Firth, J. V., 1989. Biometric analysis of Eocene and Oligocene calcareous nannofossils [Ph.D. dissert.]. Florida State Univ., Tallahassee.
- Fryer, P., Pearce, J. A., Stokking, L. B., et al., 1990. *Proc. ODP, Init. Repts.*, 125: College Station, TX (Ocean Drilling Program).
- Gallagher, L., 1989. *Reticulofenestra*: a critical review of taxonomy, structure and evolution. In Crux, J. A., and Van Heck, S. E. (Eds.), *Nannofossils and Their Application*: Chichester (Ellis Horwood), 41–75.
- Gartner, S., Chen, M. P., and Stanton, R. J., 1983. Late Neogene nannofossil biostratigraphy and paleoceanography of the northeastern Gulf of Mexico and adjacent areas. *Mar. Micropaleontol.*, 8:17–50.
- Loeblich, A. R., and Tappan, H., 1966. Annotated index and bibliography of the calcareous nannoplankton. *Phycologia*, 5:81–215.
- , 1968. Annotated index and bibliography of the calcareous nannoplankton II. *J. Paleontol.*, 42:584–598.
- , 1969. Annotated index and bibliography of the calcareous nannoplankton III. *J. Paleontol.*, 43:568–588.
- , 1970a. Annotated index and bibliography of the calcareous nannoplankton IV. *J. Paleontol.*, 44:558–574.
- , 1970b. Annotated index and bibliography of the calcareous nannoplankton V. *Phycologia*, 9:157–174.
- , 1971. Annotated index and bibliography of the calcareous nannoplankton VI. *Phycologia*, 10:315–339.
- , 1973. Annotated index and bibliography of the calcareous nannoplankton VII. *J. Paleontol.*, 47:715–759.
- Lowrie, W., Alvarez, W., Napoleone, G., Perch-Nielsen, K., Premoli Silva, I., and Toumarkine, M., 1982. Paleogene magnetic stratigraphy in Umbrian pelagic carbonate rocks: the Contessa section, Gubbio. *Geol. Soc. Am. Bull.*, 93:411–432.
- Martini, E., 1971. Neogene silicoflagellates from the equatorial Pacific. In Winterer, E. L., Riedel, W. R., et al., *Init. Repts. DSDP*, 7 (Pt. 2): Washington (U.S. Govt. Printing Office), 1695–1708.
- Martini, E., 1980. Oligocene to Recent calcareous nannoplankton from the Philippine Sea, Deep Sea Drilling Project Leg 59. In Kroenke, L., Scott, R., et al., *Init. Repts. DSDP*, 59: Washington (U.S. Govt. Printing Office), 547–566.
- Martini, E., and Bramlette, M. N., 1963. Calcareous nannoplankton from the experimental Mohole drilling. *J. Paleontol.*, 37:845–856.
- Müller, C., 1970. Nannoplankton aus dem Mittel-Oligozän von Norddeutschland und Belgien. *Neues Jahrb. Geol. Paläontol. Abh.*, 135:82–101.
- , 1974. Calcareous nannoplankton, Leg 25 (Western Indian Ocean). In Simpson, E.S.W., Schlich, R., et al., *Init. Repts. DSDP*, 25: Washington (U.S. Govt. Printing Office), 579–634.
- Okada, H., and Bukry, D., 1980. Supplementary modification and introduction of code numbers to low-latitude coccolith biostratigraphic zonation (Bukry, 1973; 1975). *Mar. Micropaleontol.*, 5:321–325.
- Olafsson, G., 1989. Oligocene/Miocene morphometric variability of the *Cyclicargolithus* lineage from the equatorial Atlantic and Indian oceans. *INA News.*, 11:85.
- Perch-Nielsen, K., 1985. Cenozoic calcareous nannofossils. In Bolli, H. M., Saunders, J. B., and Perch-Nielsen, K. (Eds.), *Plankton Stratigraphy*: Cambridge (Cambridge Univ. Press), 427–554.

- Pujos-Lamy, A., 1987. Eocene to Pleistocene medium-sized and small-sized "Reticulofenestrids." *Abh. Geol. Bundesanst. Austria*, 39:239-277.
- Steinmetz, J. C., 1985a. Bibliography and taxa of calcareous nannoplankton—V. *INA Newsl.*, 7:5-28.
- , 1985b. Bibliography and taxa of calcareous nannoplankton—VI. *INA Newsl.*, 7:122-145.
- , 1986. Bibliography and taxa of calcareous nannoplankton—VIII. *INA Newsl.*, 8:66-87.
- , 1987a. Bibliography and taxa of calcareous nannoplankton—IX. *INA Newsl.*, 9:6-29.
- , 1987b. Bibliography and taxa of calcareous nannoplankton—X. *INA Newsl.*, 10:81-109.
- , 1988a. Bibliography and taxa of calcareous nannoplankton—XI. *INA Newsl.*, 10:7-28.
- , 1988b. Bibliography and taxa of calcareous nannoplankton—XII. *INA Newsl.*, 10:60-88.
- , 1989. Bibliography and taxa of calcareous nannoplankton—XIII. *INA Newsl.*, 11:6-23.
- van Heck, S. E., 1979a. Bibliography and taxa of calcareous nannoplankton. *INA Newsl.*, 1:AB1-B27.
- , 1979b. Bibliography and taxa of calcareous nannoplankton. *INA Newsl.*, 1:ABV1-B42.
- , 1980a. Bibliography and taxa of calcareous nannoplankton. *INA Newsl.*, 2:5-34.
- , 1980b. Bibliography and taxa of calcareous nannoplankton. *INA Newsl.*, 2:43-81.
- , 1981a. Bibliography and taxa of calcareous nannoplankton. *INA Newsl.*, 3:4-41.
- , 1981b. Bibliography and taxa of calcareous nannoplankton. *INA Newsl.*, 3:51-86.
- , 1982a. Bibliography and taxa of calcareous nannoplankton. *INA Newsl.*, 4:7-50.
- , 1982b. Bibliography and taxa of calcareous nannoplankton. *INA Newsl.*, 4:65-96.
- , 1983. Bibliography and taxa of calcareous nannoplankton. *INA Newsl.*, 5:4-13.
- Wei, W., and Wise, S. W., Jr., 1989. Paleogene calcareous nannofossil magnetobiochronology: results from South Atlantic DSDP Site 516. *Mar. Micropaleontol.*, 14:119-152.
- , 1990. Middle Eocene-Oligocene calcareous nannoplankton biogeographic gradient of the South Atlantic Ocean. *Palaeogeogr. Palaeoclimatol., Palaeoecol.*, 79:29-62.
- Clauisococcus fenestratus* (Deflandre and Fert) Prins, 1979. (Pl. 3, Figs. 3-4)
- Coccolithus eopelagicus* (Bramlette and Riedel) Bramlette and Sullivan, 1961.
- C. formosus* (Kamptner) Wise, 1973. (Pl. 3, Figs. 1-2)
- C. miopelagicus* Bukry, 1971.
- C. pelagicus* (Wallich) Schiller, 1930.
- Coccolithus staurion* Bramlette and Sullivan, 1961. (Pl. 2, Figs. 10, 13)
- Coronocylus nitescens* (Kamptner) Bramlette and Wilcoxon, 1967.
- Cyclicargolithus floridanus* (Roth and Hay) *abisectus* (Müller) n. comb. (Pl. 3, Figs. 7-8; Pl. 4, Fig. 14)
- C. floridanus floridanus* (Roth and Hay) Bukry, 1971. (Pl. 3, Figs. 9-10; Pl. 4, Fig. 15)
- Dictyococcites daviesii* (Haq) Perch-Nielsen, 1971.
- D. scrippsae* Bukry and Percival, 1971.
- Discoaster archipelagoensis* Singh and Vimal, 1976.
- D. asymmetricus* Gartner, 1969.
- D. aulakos* Gartner, 1967.
- D. barbadiensis* Tan, 1972. (Pl. 2, Fig. 2)
- D. berggrenii* Bukry, 1971.
- D. bifax* Bukry, 1971.
- D. binodosus* Martini, 1958.
- D. blackstockae* Bukry, 1973.
- D. brouweri* Tan emend. Bramlette and Riedel, 1954. (Pl. 5, Fig. 12)
- D. calcaris* Gartner, 1967. (Pl. 5, Fig. 13)
- D. challengerii* Bramlette and Riedel, 1954.
- D. decorus* (Bukry) Bukry, 1973.
- D. deflandrei* Bramlette and Riedel, 1954.
- D. delicatus* Bramlette and Sullivan, 1961.
- D. divaricatus* Hay, 1967.
- D. druggii* Bramlette and Wilcoxon, 1967.
- D. exilis* Martini and Bramlette, 1963.
- D. hamatus* Martini and Bramlette, 1963. (Pl. 5, Fig. 11)
- D. intercalaris* Bukry, 1971.
- D. kugleri* Martini and Bramlette, 1963.
- D. pansus* (Bukry and Percival) Bukry, 1973.
- D. pentaradiatus* Tan emend. Bramlette and Riedel, 1954.
- D. quinquenarius* Gartner, 1969. (Pl. 4, Fig. 1)
- D. saipanensis* Bramlette and Riedel, 1954. (Pl. 2, Fig. 1)
- D. sanmiguelensis* Bukry, 1981.
- D. stellulus* Gartner, 1967.
- D. subdeflandrei* Furrzola and Iturralde, 1967.
- D. surculus* Martini and Bramlette, 1963.
- D. tani* Bramlette and Riedel, 1954.
- D. tani nodifer* Bramlette and Riedel, 1954.
- D. triradiatus* Tan, 1927.
- D. variabilis* Martini and Bramlette, 1963.
- Helicosphaera burkei* Black, 1971.
- H. carteri* (Wallich) Kamptner, 1954.
- H. compacta* Bramlette and Wilcoxon, 1967. (Pl. 4, Figs. 4-5)
- H. dinesenii* Perch-Nielsen, 1954.
- H. euphratis* Haq, 1954. (Pl. 4, Figs. 2-3)
- H. granulata* Bukry and Percival, 1971.
- H. heezenii* Bukry, 1971.
- H. kamptneri* Hay and Mohler, 1967. (Pl. 4, Figs. 6-7)
- H. oblique* Bramlette and Wilcoxon, 1967.
- H. recta* Haq, 1966.
- H. scissura* Müller, 1981.
- H. sellii* Bukry and Bramlette, 1969.
- H. seminulum* Bramlette and Sullivan, 1961.
- H. wallichii* (Lohmann) Boudreaux and Hay, 1969.
- H. wilcoxonii* Gartner, 1971.
- Isthmolithus recurvus* Deflandre, 1954.
- Lanternithus minutus* Stradner, 1962.
- Markalius inversus* (Deflandre) Bramlette and Martini, 1964.
- Nannotetrina cristata* (Martini) Perch-Nielsen, 1971.
- Pontosphaera multipora* (Kamptner) Roth, 1970.
- Reticulofenestra bisecta* (Hay, Mohler, and Wise) Roth, 1970. (Pl. 3, Figs. 13-14; Pl. 4, Fig. 8)
- R. hillae* Bukry and Percival, 1954.
- R. minuta* Roth, 1970.
- R. minutula* (Gartner) Haq and Berggren, 1978.
- R. onusta* (Perch-Nielsen) Wise, 1983. (Pl. 1, Fig. 9)
- R. pseudumbilica* (Gartner) Gartner, 1969.
- R. reticulata* (Gartner and Smith) Roth and Thierstein, 1972. (Pl. 2, Figs. 8-9)
- R. samodurovii* (Hay, Mohler, and Wade) Roth, 1970. (Pl. 2, Fig. 11)

Date of initial receipt: 5 July 1990

Date of acceptance: 24 July 1991

Ms 125B-142

APPENDIX

Calcareous nannofossils considered in this paper are here given in alphabetic order of species epithets.

- Amaurolithus delicatus* Gartner and Bukry, 1971. (Pl. 5, Figs. 3-4)
- A. primus* (Bukry and Percival) Gartner and Bukry, 1975.
- A. tricorniculatus* (Gartner) Gartner and Bukry, 1975. (Pl. 5, Figs. 1-2)
- Blackites spinosus* (Deflandre and Fert) Hay and Towe, 1962.
- Calcidiscus leptoporus* (Murray and Blackman) Loeblich and Tappan, 1978.
- C. macintyreii* (Bukry and Bramlette) Loeblich and Tappan, 1978. (Pl. 4, Fig. 9)
- C. protoannulus* (Gartner) Loeblich and Tappan, 1978.
- Campylosphaera dela* (Bramlette and Sullivan) Hay and Mohler, 1967. (Pl. 1, Fig. 8)
- Catinaster calyculus* Martini and Bramlette, 1963. (Pl. 5, Figs. 5-6)
- C. coalitus* Martini and Bramlette, 1963. (Pl. 5, Figs. 9-10, 17)
- C. mexicanus* Bukry, 1971. (Pl. 5, Figs. 7-8, 18)
- C. umbrellus* Bukry, 1971.
- Chiasmolithus altus* Bukry and Percival, 1971. (Pl. 2, Figs. 4-5)
- C. californicus* (Sullivan) Hay and Mohler, 1967.
- C. consuetus* (Bramlette and Sullivan) Hay and Mohler, 1967.
- C. expansus* (Bramlette and Sullivan) Garter, 1970. (Pl. 1, Figs. 1-2, 10)
- C. grandis* (Bramlette and Riedel) Radomski, 1968. (Pl. 1, Figs. 3-4, 7)
- C. oamaruensis* (Deflandre) Hay, Mohler and Wise, 1966. (Pl. 1, Figs. 5-6; Pl. 2, Figs. 6-7)
- C. solitus* (Bramlette and Sullivan) Locker, 1968. (Pl. 2, Fig. 12)

- R. umbilica* (Levin) Martini and Ritzkowski, 1968. (Pl. 3, Figs. 11–12)
Rhabdosphaera claviger Murray and Blackman, 1898.
Scyphosphaera aranta Kamptner, 1967.
Sphenolithus abies Deflandre, 1954.
S. celsus Haq, 1971.
S. ciproensis Bramlette and Wilcoxon, 1967. (Pl. 3, Figs. 5–6)
S. conicus Bukry, 1971.
S. delphix Bukry, 1973.
S. distentus (Martini) Bramlette and Wilcoxon, 1967. (Pl. 3, Figs. 15–16, 19)
S. furcatolithoides Locker 1967.
S. heteromorphus Deflandre, 1953. (Pl. 5, Fig. 16)
S. intercalaris Martini, 1976.
- S. moriformis* (Brönnimann and Stradner) Bramlette and Wilcoxon, 1967.
S. obtusus Bukry, 1971.
S. predistentus Bramlette and Wilcoxon, 1967. (Pl. 3, Figs. 17–18, 20)
S. primus Perch-Nielsen, 1971.
S. pseudoradians Bramlette and Wilcoxon, 1967. (Pl. 2, Fig. 3)
S. radians Deflandre, 1952.
S. spiniger Bukry, 1971.
Triquetrorhabdulus carinatus Martini, 1965. (Pl. 4, Figs. 12–13)
T. millowii Bukry, 1971. (Pl. 4, Figs. 10–11)
T. rugosus Bramlette and Wilcoxon, 1967. (Pl. 5, Figs. 14–15)
Umbilicosphaera sibogae (Weber-Van Bosse) Gartner, 1970.
Zygrhablithus bijugatus (Deflandre) Deflandre, 1959.

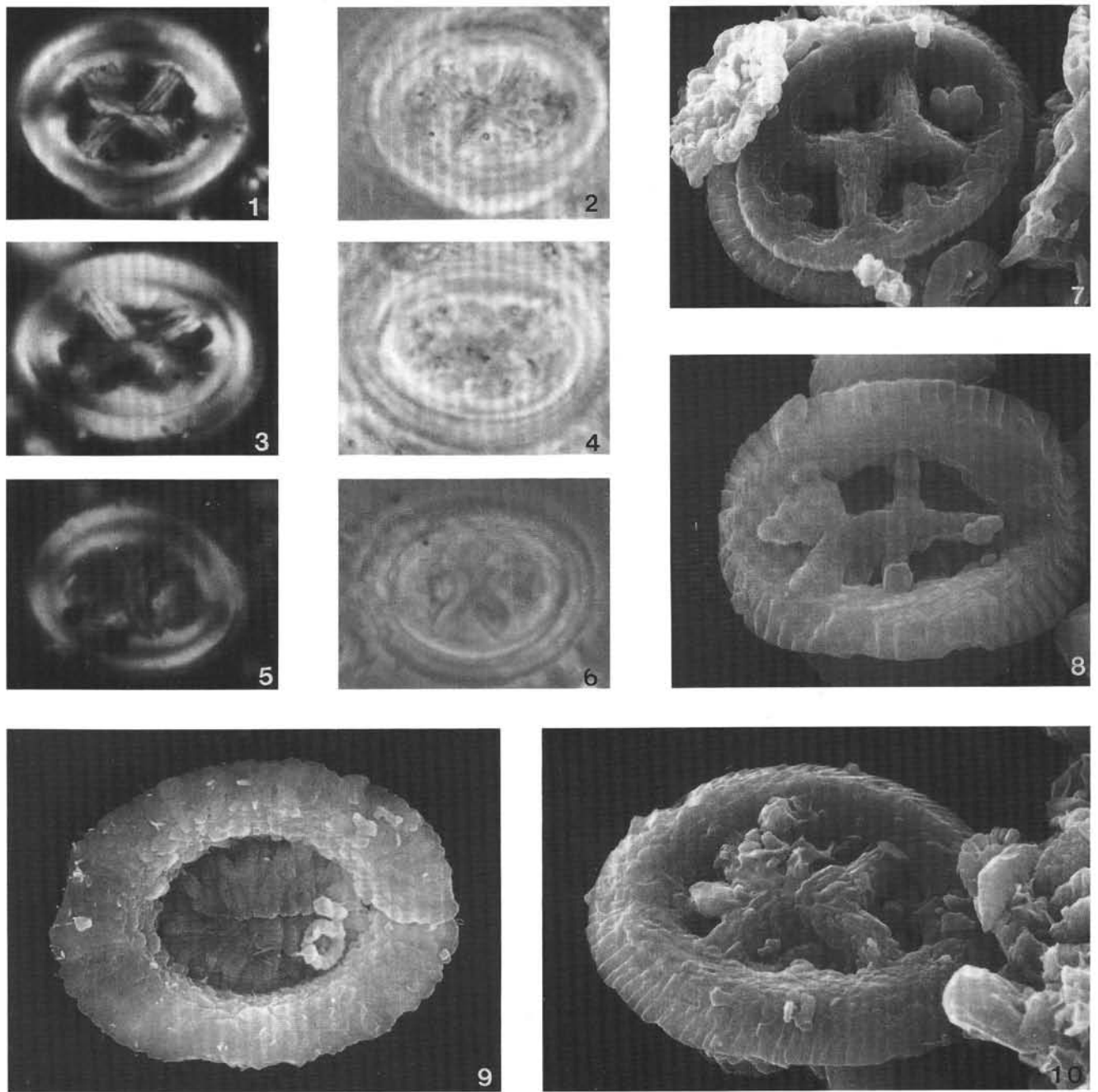


Plate 1. Eocene calcareous nannofossils. 1–2. *Chiasmolithus expansus* (Bramlette and Sullivan) Gartner, Sample 125-786A-11X-4, 62–63 cm, $\times 1560$. (1) cross-polarized light. (2) phase contrast light. 3–4. *Chiasmolithus grandis* (Bramlette and Riedel, etc.) Radomski, Sample 125-786A-11X-4, 62–63 cm, $\times 1560$. (3) cross-polarized light. (4) phase contrast light. 5–6. *Chiasmolithus oamaruensis* (Deflandre) Hay, Mohler, and Wade, Sample 125-782A-40X-4, 16–17 cm, $\times 1560$. (5) cross-polarized light. (6) phase contrast light. 7. *Chiasmolithus grandis* (Bramlette and Riedel) Radomski, Sample 125-782A-42X-1, 72–73 cm, distal view, $\times 2700$, SEM. 8. *Campylosphaera dela* (Bramlette and Sullivan) Hay and Mohler, Sample 125-782A-42X-1, 72–73 cm, distal view, $\times 4300$, SEM. 9. *Reticulofenestra onusta* (Perch-Nielsen) Wise, Sample 125-782A-42X-1, 72–73 cm, distal view, $\times 3000$, SEM. 10. *Chiasmolithus expansus* (Bramlette and Sullivan) Gartner, Sample 125-782A-42X-1, 72–73 cm, distal view, $\times 4000$, SEM.

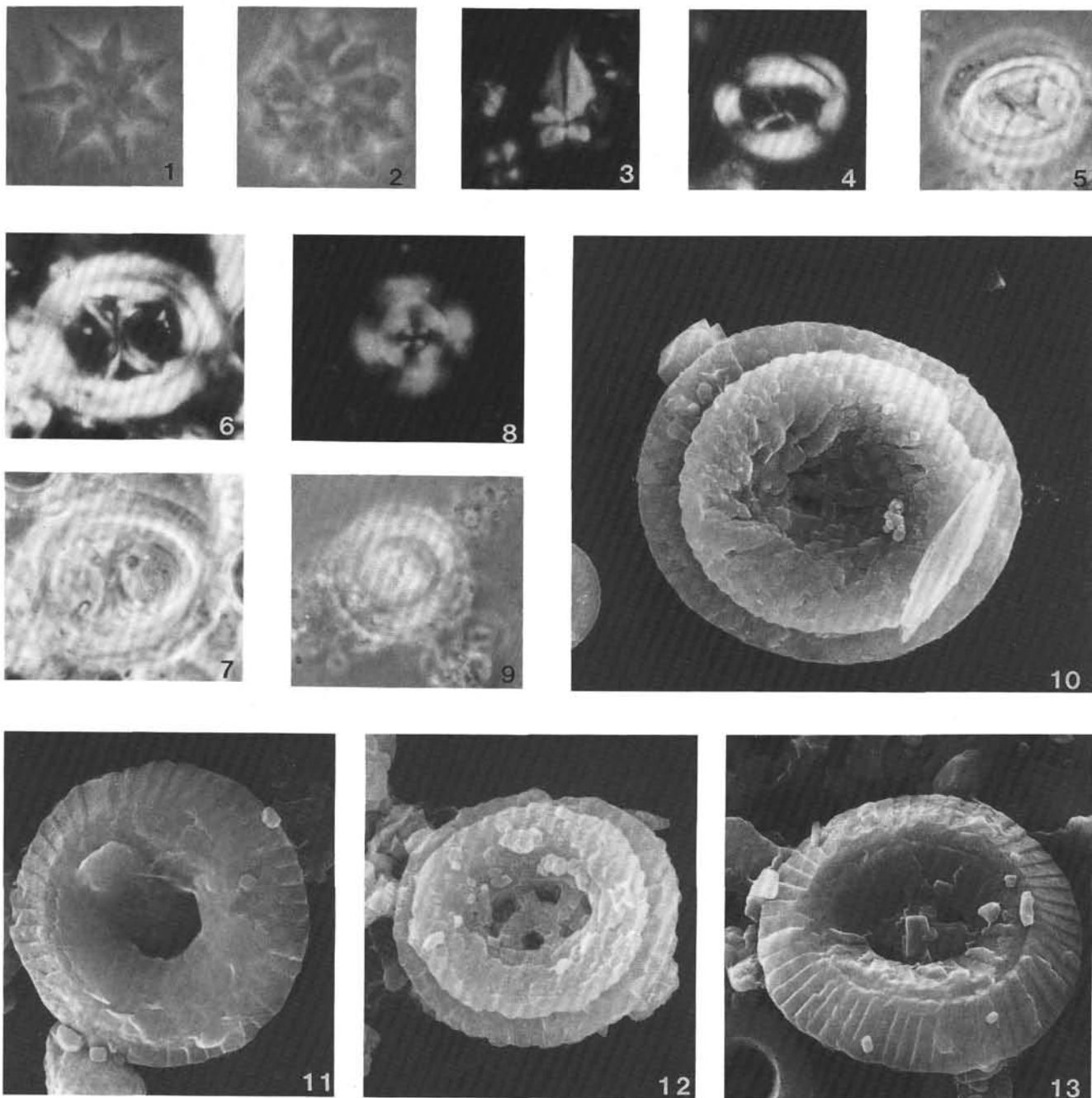


Plate 2. Eocene calcareous nannofossils. **1.** *Discoaster saipanensis* Bramlette and Riedel, Sample 125-786A-11X-2, 62–64 cm, $\times 1560$, phase contrast light. **2.** *Discoaster barbadiensis* Tan, Sample 125-782A-40X-CC, $\times 1560$, phase contrast light. **3.** *Sphenolithus pseudoradians* Bramlette and Wilcoxon, Sample 125-786A-11X-1, 8–10 cm, $\times 1560$, cross-polarized light. **4–5.** *Chiasmolithus altus* Bukry and Percival, Sample 125-786A-10X-3, 14–15 cm, $\times 1560$. (4) cross-polarized light. (5) phase contrast light. **6–7.** *Chiasmolithus oamaruensis* (Deflandre) Hay, Mohler, and Wade, Sample 125-786A-11X, 8–10 cm, $\times 1560$. (6) cross-polarized light. (7) phase contrast light. **8–9.** *Reticulofenestra reticulata* (Gartner and Smith) Roth and Thierstein, Sample 125-786A-11X-1, 54–55 cm, $\times 1560$. (8) cross-polarized light. (9) phase contrast light. **10.** *Coccolithus staurion* Bramlette and Sullivan, Sample 125-782A-42X-1, 72–73 cm, proximal view, $\times 3700$, SEM. **11.** *Reticulofenestra samodurovii* (Hay, Mohler, and Wise) Roth, Sample 125-782A-41X-7, 11–12 cm, distal view, $\times 6500$, SEM. **12.** *Chiasmolithus solitus* (Bramlette and Sullivan) Locker, Sample 125-782A-42-1, 72–73 cm, distal view, $\times 3700$, SEM. **13.** *Coccolithus staurion* Bramlette and Sullivan, Sample 125-782A-41X-7, 11–12 cm, distal view, $\times 4000$, SEM.

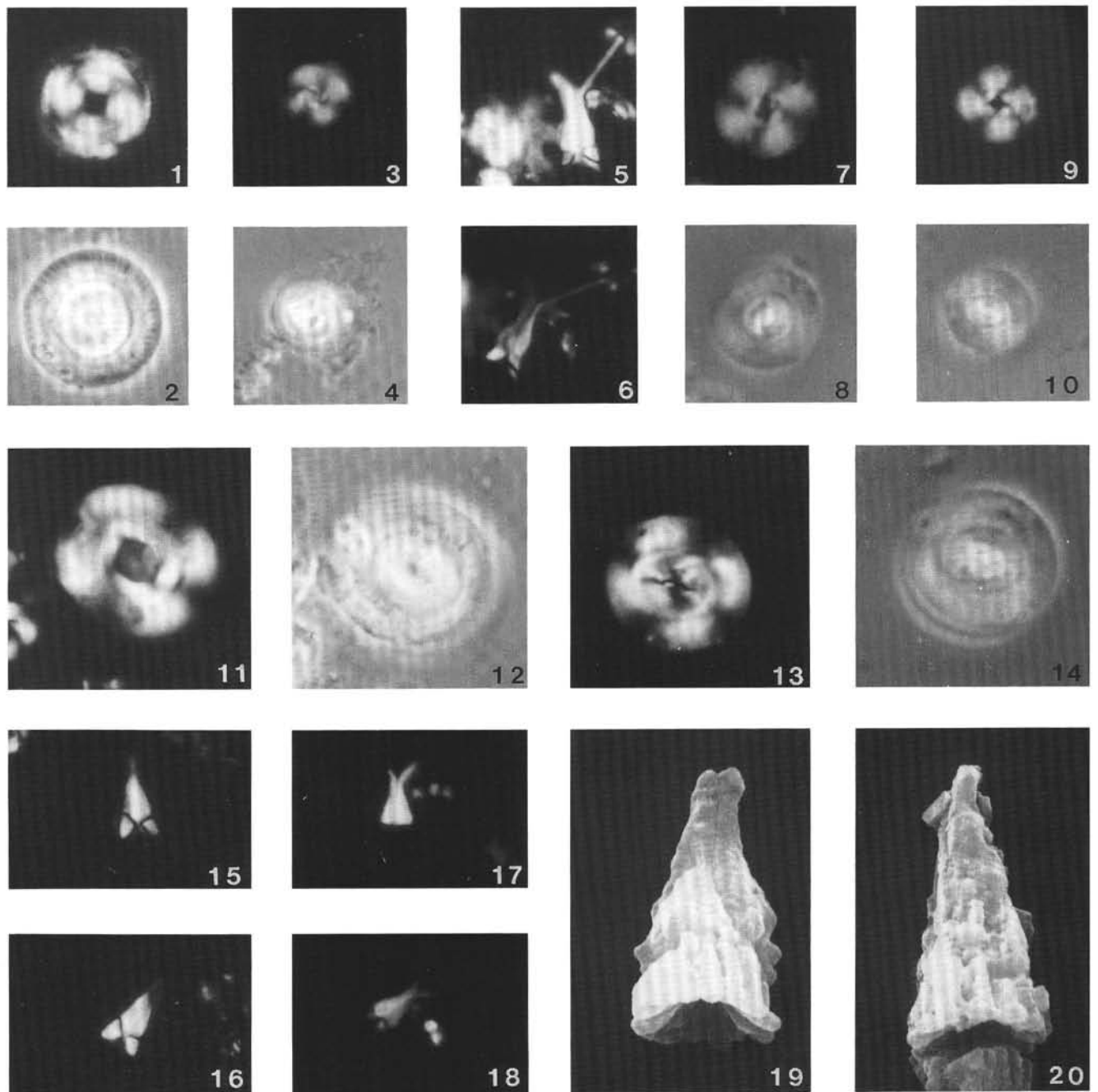


Plate 3. Oligocene calcareous nannofossils. **1–2.** *Coccolithus formosus* (Kamptner) Wise, Sample 125-786A-10X-6, 14–15 cm, $\times 1560$. (1) cross-polarized light. (2) phase contrast light. **3–4.** *Clausiococcus fenestratus* (Deflandre and Fert) Prins, Sample 125-786A-10X-6, 14–15 cm, $\times 1560$. (3) cross-polarized light. (4) phase contrast light. **5–6.** *Sphenolithus ciperoensis* Bramlette and Wilcoxon, Sample 125-782A-37X-1, 61–62 cm, $\times 1560$. (5) view parallel to cross-polarized light. (6) view at 45° to cross-polarized light. **7–8.** *Cyclicargolithus f. abisectus* (Müller) n. comb., Sample 125-782A-35X-5, 120–121 cm, $\times 1560$. (7) cross-polarized light. (8) phase contrast light. **9–10.** *Cyclicargolithus f. floridanus* (Roth and Hay) Bukry, Sample 125-782A-33X-1, 115–119 cm, $\times 1560$. (9) cross-polarized light. (10) phase contrast light. **11–12.** *Reticulofenestra umbilica* (Levin) Martini and Ritzkowski, Sample 125-786A-10X-6, 14–15 cm, $\times 1560$. (11) cross-polarized light. (12) phase contrast light. **13–14.** *Reticulofenestra bisecta* (Hay, Mohler, and Wade) Roth, Sample 125-782A-35X-CC, $\times 1560$. (13) cross-polarized light. (14) phase contrast light. **15–16.** *Sphenolithus distentus* (Martini) Bramlette and Wilcoxon, Sample 125-782A-37X-1, 62–63 cm, $\times 1560$. (15) view parallel to cross-polarized light. (16) view at 45° to cross polarized light. **17–18.** *Sphenolithus predistentus* Bramlette and Wilcoxon, Sample 125-782A-37X-2, 108–109 cm, $\times 1560$. (17) view parallel to cross-polarized light. (18) view at 45° to cross-polarized light. **19.** *Sphenolithus distentus* (Martini) Bramlette and Wilcoxon, Sample 125-782A-37X-1, 61–62 cm, $\times 7500$, SEM. **20.** *Sphenolithus predistentus* Bramlette and Wilcoxon, Sample 125-782A-37X-1, 61–62 cm, $\times 8500$, SEM.

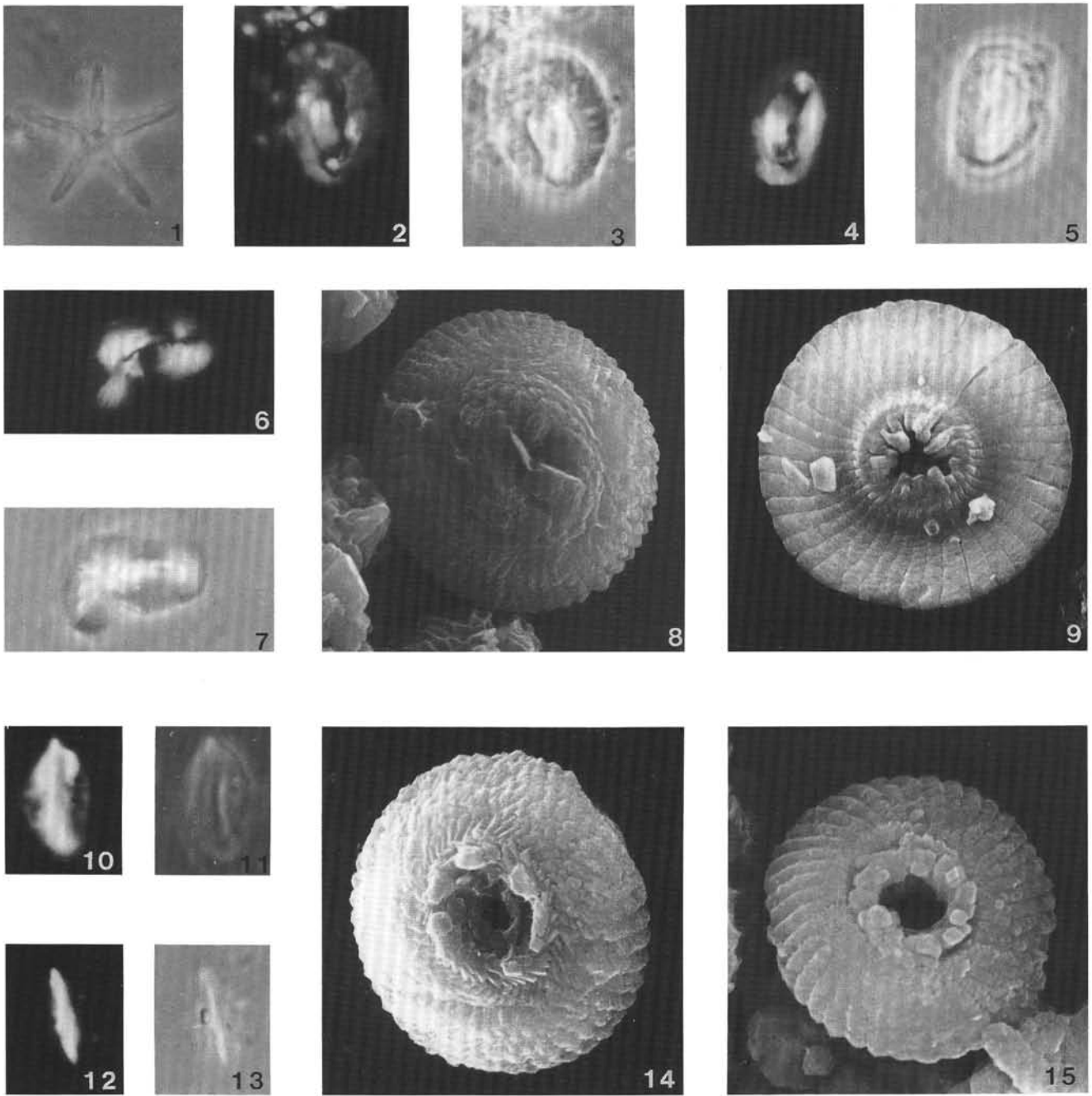


Plate 4. Oligocene to Miocene calcareous nannofossils. **1.** *Discoaster quinqueramus* Gartner, Sample 125-786A-10X-CC, $\times 1560$, phase contrast light. **2-3.** *Helicosphaera euphratis* Haq, Sample 125-786A-10X-6, 14–15 cm, $\times 1560$. (2) cross-polarized light. (3) phase contrast light. **4-5.** *Helicosphaera compacta* Bramlette and Wilcoxon, Sample 125-786A-10X-6, 14–15 cm, $\times 1560$. (4) cross-polarized light. (5) phase contrast light. **6-7.** *Helicosphaera kamptneri* Hay and Mohler, Sample 125-782A-28X-5, 37–38 cm, $\times 1560$. (6) cross-polarized light. (7) phase contrast light. **8.** *Reticulofenestra bisecta* (Hay, Mohler, and Wise) Roth, Sample 125-786A-10X-CC, distal view, $\times 6000$, SEM. **9.** *Calcidiscus macintyreii* (Bukry and Bramlette) Loeblich and Tappan, Sample 125-782A-26X-6, 91–93 cm, proximal view, $\times 4500$, SEM. **10-11.** *Triquetrorhabdulus milowii* Bukry, Sample 125-782A-35X-CC, $\times 1560$. (10) cross-polarized light. (11) phase contrast light. **12-13.** *Triquetrorhabdulus carinatus* Martini, Sample 125-782A-37X-2, 108–109 cm, $\times 1560$. (12) cross-polarized light. (13) phase contrast light. **14.** *Cyclicargolithus f. abisectus* (Müller) n. comb., Sample 125-782A-37X-2, 108–109 cm, distal view, $\times 5500$, SEM. **15.** *Cyclicargolithus f. floridanus* (Roth and Hay) Bukry, Sample 125-782A-37X-1, 61–62 cm, distal view, $\times 8500$, SEM.

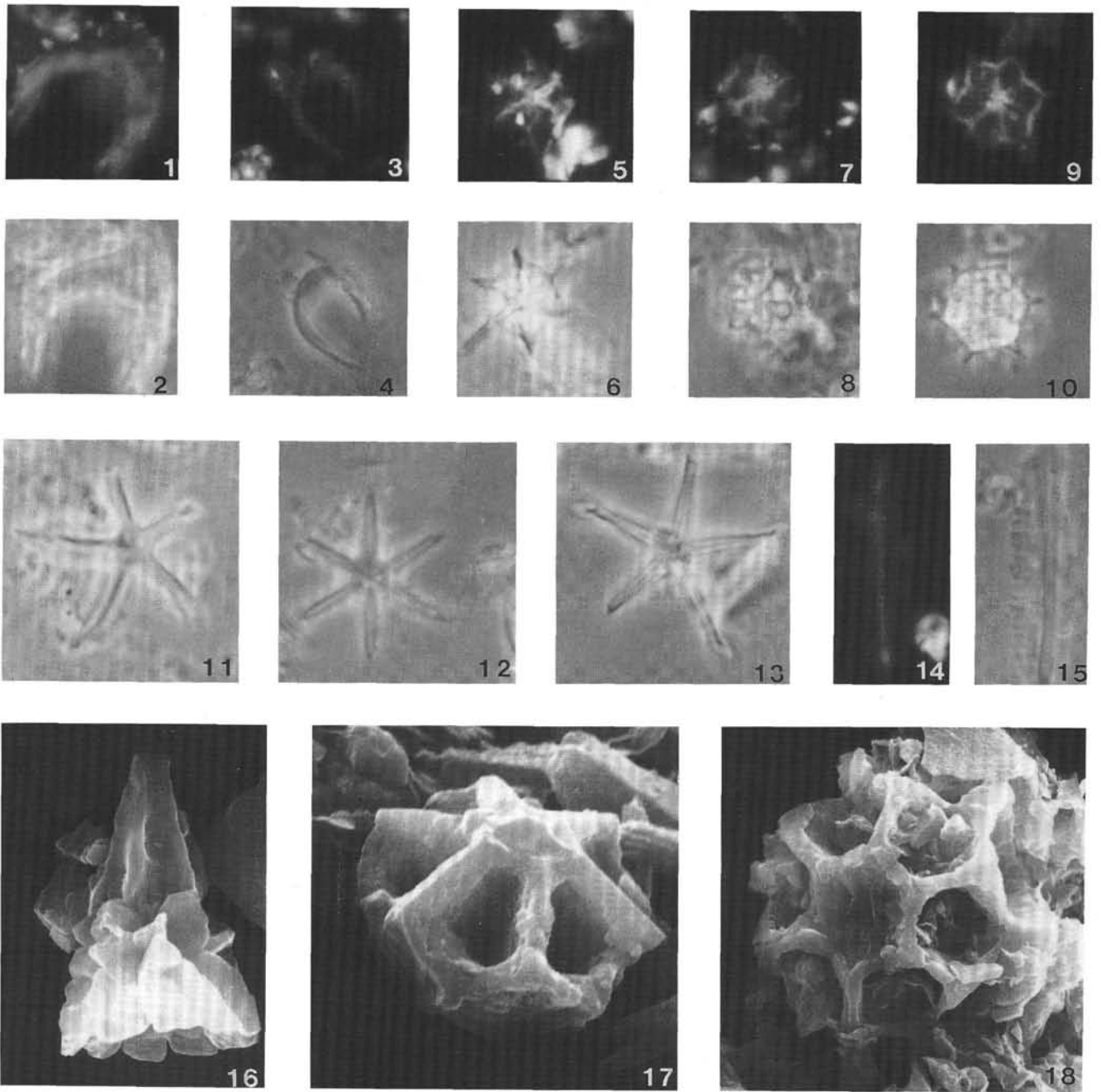


Plate 5. Miocene calcareous nannofossils. **1–2.** *Amaurolithus tricorniculatus* (Gartner) Gartner and Bukry, Sample 125-782A-18X-CC, $\times 1560$. (1) cross-polarized light. (2) phase contrast light. **3–4.** *Amaurolithus delicatus* Gartner and Bukry, Sample 125-782A-18X-CC, $\times 1560$. (3) cross-polarized light. (4) phase contrast light. **5–6.** *Catinaster calyculus* Martini and Bramlette, Sample 125-782A-26X-4, 92–93 cm, $\times 1560$. (5) cross-polarized light. (6) phase contrast light. **7–8.** *Catinaster mexicanus* Bukry, Sample 125-782A-26X-4, 92–93 cm, $\times 1560$. (7) cross-polarized light. (8) phase contrast light. **9–10.** *Catinaster coalitus* Martini and Bramlette, Sample 125-782A-26X-5, 92–93 cm, $\times 1560$. (9) cross-polarized light. (10) phase contrast light. **11.** *Discoaster hamatus* Martini and Bramlette, Sample 125-782A-26X-4, 92–93 cm, $\times 1560$, phase contrast light. **12.** *Discoaster brouweri* Tan emend. Bramlette and Riedel, Sample 125-782A-17X-1, 92–93 cm, $\times 1560$, phase contrast. **13.** *Discoaster calcaris* Gartner, Sample 125-782A-26X-4, 92–93 cm, $\times 1560$, phase contrast. **14–15.** *Triquetrorhabdulus rugosus* Bramlette and Wilcoxon, Sample 125-782A-17X-1, 92–93 cm, $\times 1560$. (14) cross-polarized light. (15) phase contrast light. **16.** *Sphenolithus heteromorphus* Deflandre, Sample 125-782A-35X-1, 83–84 cm, $\times 5500$, SEM. **17.** *Catinaster coalitus* Martini and Bramlette, Sample 125-782A-26X-6, 92–93 cm, distal view, $\times 6500$, SEM. **18.** *Catinaster mexicanus* Bukry, Sample 125-782A-26X-4, 92–93 cm, distal view, $\times 3700$, SEM.